

ISOTHERMAL MODEL OF ICF BURN WITH FINITE ALPHA RANGE TREATMENT

by

CONNER DANIEL GALLOWAY

SUBMITTED TO THE DEPARTMENT OF NUCLEAR SCIENCE AND ENGINEERING
IN PARTIAL FULFILLMENT OF THE REQUIREMENTS FOR THE DEGREES OF

BACHELOR OF SCIENCE IN NUCLEAR SCIENCE AND ENGINEERING

and

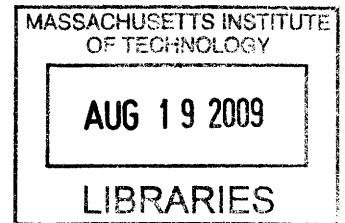
MASTER OF SCIENCE IN NUCLEAR SCIENCE AND ENGINEERING

at the

MASSACHUSETTS INSTITUTE OF TECHNOLOGY


June 2009

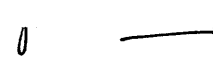
© Conner Daniel Galloway, MMIX. All rights reserved.



The author hereby grants to MIT permission to reproduce and distribute publicly paper and electronic copies of this thesis document in whole or in part.

Author ...
 Department of Nuclear Science and Engineering
May 22, 2009

Certified by ...
 Kim Molvig
Associate Professor of Nuclear Science and Engineering
Thesis Supervisor

Certified by ...
 Abhay Kumar Ram
Principal Research Scientist, Plasma Science and Fusion Center
Thesis Reader

Accepted by ...
 Jacquelyn C. Yanch
Chair, Department Committee on Graduate Students

ARCHIVES

Isothermal Model of ICF Burn with Finite Alpha Range Treatment

by

Conner Daniel Galloway

Submitted to the Department of Nuclear Science and Engineering
on May 22, 2009, in partial fulfillment of the
requirements for the degrees of
Bachelor of Science in Nuclear Science and Engineering
and
Master of Science in Nuclear Science and Engineering

Abstract

A simple model for simulating deuterium tritium burn in inertial confinement fusion capsules is developed. The model, called the Isothermal Rarefaction Model, is zero dimensional (represented as ordinary differential equations) and treats disassembly in the isothermal limit. Two substantive theoretical developments are contained in this model; one is an improved treatment of fast alpha slowing down, and the other is a calculation of the fusion product source distributions and their energy moment. The fast alpha stopping treatment contains a derivation of the Fraley fractional energy splitting functional form, $f_e = 1/(1 + xT_e)$, resulting in an expression for the numerical factor x which will be defined as the Fraley parameter. The average thermal energy which is lost from the thermal ion distribution when two particles fuse is found from the energy moment of the fusion product source distribution. This energy contributes to the energy of the fusion products. A third theoretical development that is discussed for completeness and future use, but not yet incorporated in the Isothermal Rarefaction Model, is the 4T theory of matter-radiation energy exchange in homogenous optically thick media. The isothermal rarefaction model assumes an optically thin to marginally thick plasma, and only Bremsstrahlung emission and absorption are treated in this thesis. The 4T theory for optically thick media has been published. A sampling of results using the Isothermal Rarefaction Model is presented.

Thesis Supervisor: Kim Molvig

Title: Associate Professor of Nuclear Science and Engineering

Thesis Reader: Abhay Kumar Ram

Title: Principal Research Scientist, Plasma Science and Fusion Center

Acknowledgments

I would like to thank Kim Molvig and Marv Alme for all of their help, guidance, and many enlightening conversations.

Contents

1	Introduction	11
2	Isothermal Rarefaction Model	12
3	Burn Physics	18
3.1	Reactivity	19
3.2	Rate of Energy Loss From Thermal Distribution Due to Fusion	20
3.3	Distribution of Fusion Products	24
4	Finite Alpha Range	30
4.1	Slowing Down Equation	31
4.2	Limits and Approximations	35
4.3	Geometry	42
5	Radiation	47
6	Simulation Results of the Isothermal Rarefaction Model	54
7	Conclusion	65

List of Figures

1	Geometry for calculating fusion particle source distribution.	26
2	Range of fast alpha particles in a homogenous medium. The red curve is calculated assuming only collisions with electrons. The black curve is calculated assuming collisions with both electrons and ions, but the appropriate limits of the Chandresekhar functions have been taken. The blue curve is calculated the same as the black, but without the simplifications of the Chandresekhar functions and with $T_i = 10$ KeV.	38
3	Fraction of fast alpha particle energy given to the plasma electrons. The green curve is the well known Fraley result. The red curve is calculated from eq.(159). The black curve is calculated numerically.	41
4	The geometry for the calculation of the fraction of fast alpha energy that leaves the fuel sphere.	44
5	Ion and Electron Temperature Profiles	57
6	Radius of Incoming Rarefaction Wave	57
7	Densities (g/cm^3) of deuterium and tritium fuel ions and thermalized alpha particles	58
8	Burn Up Fraction	58
9	Fraction of fast alpha particles that are deposited in the fuel sphere (blue). Fraction of total instantaneous fusion power delivered to electrons (green). Fraction of total instantaneous fusion power delivered to ions (red).	59
10	Ion and Electron Temperature Profiles	60
11	Radius of Incoming Rarefaction Wave	61
12	Densities (g/cm^3) of deuterium and tritium fuel ions and thermalized alpha particles	61

13	Burn Up Fraction	62
14	Fraction of fast alpha particles that are deposited in the fuel sphere (blue). Fraction of total instantaneous fusion power delivered to electrons (green). Fraction of total instantaneous fusion power delivered to ions (red).	62
15	Burn up fractions as a function of ρR . The 5 KeV and 7 KeV initial temperature simulations were independent of initial fuel mass.	64

1 Introduction

With the recent completion of the NIF laser system, the Inertial Confinement method for controlled fusion has been brought to the front lines in fusion research. With its lasers able to deliver a few megajoules in 10-20 nanoseconds, researchers will be able to test many codes, models, and theories and perhaps achieve gains of 30-40. Like magnetic fusion, inertial fusion has been a long road with many experiments that have failed to break even. The two main laser fusion experiments which preceded NIF at Lawrence Livermore National Laboratory, Shiva and Nova, had trouble with the Rayleigh Taylor instability (which still plagues ICF), and scientists have had trouble maintaining laser focus on the imploding fuel capsules as they shrink. However, more and more progress is made daily toward the goal of developing an economical fusion reactor.

The goal of this thesis is to develop a system of ODE equations that take into account essential features of the burn of compressed ICF fuel capsules. This system can be integrated faster than most one or two dimensional radiation hydrocodes. The set of equations constitutes the Isothermal Rarefaction Model. Particular attention will be given to the theoretical development of burn physics and the treatment of fast alpha slowing down as it pertains to burning plasmas in general, as well as to the specific model developed in this thesis. The isothermal rarefaction model is intended to be used as an effective quick estimate of the performance of compressed ICF capsules.

The first section, *Isothermal Rarefaction Model*, will discuss the assumptions and details of the model, and an initial set of equations will be presented. In next section, *Burn Physics*, the dynamics of DT burn will be addressed leading to expressions for the particle and energy sinks and sources in the rate equations presented in the first section. In particular, the average energy lost from the thermal ion distribution when two particles fuse will be calculated as an integral over the cross section. This extra bit of energy is given to the fusion products in addition to the reaction Q-value. In the third section, *Finite Alpha Range*, an equation governing the slowing down of fast alpha particles will be derived, as well as approximate, but accurate, expressions for the alpha particle range, slowing down time, and fraction of energy given to the electrons. In particular, the fraction of energy given to the electrons (derived from first principles with approximations)

will be compared with the well known Fraley empirical formula $f_e = \frac{1}{1+T_e/32}$ (G. S. Fraley, E. J. Linnebur, R. J. Mason & R. L. Morse, *Phys. Fluids*, vol. 17, 474 (1974) 1974). Finally, expressions specific to the Isothermal Rarefaction Model will be derived. In the fourth section, *Radiation*, an expression for the energy loss from the model system due to radiation will be derived including re-absorption but ignoring scattering and assuming quasi-steady state for the photons. Furthermore, the radiation dynamics for an optically thick system will be discussed, although this is not assumed in the current model. Finally, in *Simulation Results of the Isothermal Rarefaction Model*, the final equations of the model as well as simulation results will be presented.

2 Isothermal Rarefaction Model

There are two main phases in ICF. The first is the implosion phase, where a driver of some kind compresses the fuel to densities of the order of 1000 times solid density and forms a lower density hot spot in the center. The second phase involves the expansion of the material where the hot spot ignites and propagates a burn wave outward through the colder dense fuel. A rarefaction wave begins to proceed inwards from the outer surface of the compressed fuel due to the expansion of the fluid into a vacuum after implosion stagnation. Once burn of the hot spot begins, which typically ignites at a few KeV, the electrons and ions in the burning fuel are heated rapidly by fast alpha particles. They are also heated by neutrons, but neutron heating is typically small because of the neutron's small mean free path. Neutron heating will be ignored in this model.

Since the ion-ion and electron-electron collision rates are fast compared to the ion-electron energy exchange rates, the ion and electrons can depart in temperature while maintaining Maxwellian distributions. At first, the fast alpha particles primarily heat the electrons. Furthermore, because the electron-ion energy exchange is fast at small T_e due to its $T_e^{-3/2}$ dependence, the ions are quickly heated as well. However once the fuel gets up to 20 keV, the ions are dominantly heated and their temperature runs away, due both to the increasing reactivity and to the drop off in their rate of cooling to the electrons. The electron's coupling to the radiation is also important. This will be discussed in the radiation section.

The electron thermal conduction coefficient becomes very large in the burning fuel because it varies with temperature as $T_e^{5/2}$. This tends to keep the electrons isothermal. At lower electron temperatures, the strong ion-electron energy coupling tends to keep the ions isothermal before runaway burn. When the ions run away at higher temperatures upwards of 100 keV, the ion thermal conduction tends to keep the ions isothermal. The heating from fusion alphas is usually fairly uniform.

It is a combination of fast alpha particles passing through the hot burning fuel (where their mean free path is longer) and depositing a large amount of their energy in the colder dense fuel (where their mean free path is smaller), and the strong conduction into the cold fuel, that propagates the burn wave. If the burn wave propagates through the colder dense fuel on a faster time scale than the rarefaction wave proceeds inwards from the outer surface, then the whole fuel quickly becomes isothermal. The speed of the burn propagation is controlled by the time scales of alpha slowing down, and electron conduction coupled through ion-electron energy relaxation. These times are typically of order 1-10 ps (Yigal Ronen Guillermo Velarde Jose M. Martinez-Val, *An Introduction to Nuclear Fusion by Inertial Confinement* (Boca Raton, Florida: CRC Press, Inc., 1993) 1993). This is the physical basis of the isothermal burn model. The specifics of the model and its assumptions will now be presented in more detail.

The isothermal rarefaction model assumes the fuel has been compressed at implosion stagnation to a homogenous sphere with a certain radius R_o , and a certain fuel density, ion temperature, and electron temperature. At the initial time in the model, the fuel begins to burn uniformly as a rarefaction wave proceeds inwards from the outer radius R_o . As soon as the rarefaction wave passes a particular fuel element, it is assumed that the density and temperature quickly fall off and that burn stops in that fuel element. At any given time, the information that the shell is rarefying has not reached fluid elements inside the rarefaction wave. These fluid elements still burn as if they were in a homogeneous medium. This is significant, as it means there is no advection or hydro motion inside the rarefaction wave. There is only burn physics, possible electron and ion conduction transporting energy into the rarefacted material, and energy lost to radiation. Once the rarefaction wave reaches the origin, the burn is over.

The classical electron conduction coefficient is (Per Helander & Dieter J. Sigmar, *Collisional Transport in Magnetized Plasmas* (Cambridge, UK: Cambridge University Press, 2002) 2002)

$$\kappa_e = n_e \chi_e = 1.185 \sqrt{\frac{2}{\pi}} \frac{c}{r_e^2 Z_{eff} \ln \Lambda_e} \left(\frac{T_e}{m_e c^2} \right)^{5/2} \quad (1)$$

where r_e is the classical electron radius and χ_e is the thermal diffusivity. An electron conduction time scale is given by

$$\tau_e = \frac{l^2}{\chi_e} \quad (2)$$

where l is a scale length for the system. The fusion time scale is given by

$$\tau_{fus} = \frac{1}{\langle \sigma v \rangle n_i} \quad (3)$$

where n_i is the number density of either the deuteron or triton populations (homogenous equal mixture assumed). Typical ICF parameters are $\ln \Lambda_e \approx 5.7$, $T_e \approx 40$ keV, $T_i \approx 70$ keV, $n_i \approx 2.5 \times 10^{25}$ #/cc, and $l \approx 0.01$ cm. The times scales compare as $\tau_f = 4.5 \times 10^{-11}$ s and $\tau_e = 2.2 \times 10^{-11}$ s. The parameters are chosen near the beginning of runaway burn, and $T_i = 70$ keV is at the peak of the reactivity. As the electron and ion temperatures continue to rise, the fusion rate will decrease while the conduction rate will increase. The electron conduction rate tends to be of the same order as the fusion time scale initially, but it is much larger than the fusion rate when burn is well underway. This gives credibility to the physical picture of the isothermal model.

The ions and electrons are assumed to be Maxwellian at different temperatures. The energy exchange rate between the ions and electrons is found by taking the energy moment of the Fokker Plank equation with two Maxwellians. The result is

$$P_{ie} = \frac{6}{\sqrt{\pi}} \nu_T \left(\frac{m_e c^2}{2T_e} \right)^{3/2} \ln(\Lambda_e) (T_i - T_e) \sum_i \frac{m_e}{m_i} Z_i^2 n_i \quad (4)$$

where $\nu_T = cn_e \sigma_T$ is the Thomson rate, and the Thompson cross section is $\sigma_T = \frac{8\pi}{3} r_e^2$, and r_e is the classical electron radius. Here the sum is over all of the ion species. This is the energy exchange rate between the ions and electrons within the homogenous sphere. The electron and ion coulomb

logarithms used in this model are taken from Atzeni(Stefano Atzeni & Jurgen Meyer-Ter-Vehn, *The Physics of Inertial Fusion* (Oxford: Oxford University Press, 2007) 2007) and are given by

$$\ln \Lambda_e = 7.1 - 0.5 \ln \frac{n_e}{10^{21}} + \ln T_e \quad (5)$$

$$\ln \Lambda_i = 9.2 - 0.5 \ln \frac{n_e}{10^{21}} + 1.5 \ln T_i \quad (6)$$

where the densities are in particles per cc and the temperatures are in KeV.

Once the whole fuel begins burning, fuel ions get destroyed and high energy alpha particles are born. The alpha particles slow down in the fuel transferring their energy along their path to ions and electrons. Some stop in the fuel while others leave the fuel and enter the rarefacted material. Once the alpha particles slow down to thermal speeds, they become part of the thermal ion distribution. Alpha particles that enter the rarefacted material are assumed lost and do not contribute the thermal ion population inside the rarefaction wave. It is assumed that the homogenous burning sphere of fuel stays quasineutral. Since the ion-ion collision rate is very large ($\tau_{ii} = 1.7 \times 10^{-12}$ s for the typical ICF parameters given above), all of the ion species are thermalized at the same temperature T_i . Finally, the electrons radiate Bremsstrahlung. If the photon Thompson mean free path is small compared to system length scales, the photon distribution can build up and approach black body. The coupling between the photons and electrons then becomes complicated with re-absorption, Thomson scattering, and even Compton scattering for large enough system scale lengths. The isothermal model assumes optically thin to marginally thick fuel, and only includes Bremsstrahlung.

Due to the isothermal assumptions, the fusion heating source terms are calculated as follows. The fast alpha slowing down time is fast compared to all other dynamic time scales. Therefore it is assumed that there is no delay between when an alpha particle is born and when it is deposited at the end of its range., ie, that there are no significant changes in n_i , T_i , T_e , or the radius of the rarefaction wave R , during the time it takes any given alpha to slow down. The amount of energy per second that all of the fast alpha particles born in the homogenous sphere (inside the rarefaction

wave) transfer to the thermal ions and electrons (also within the rarefaction wave) is calculated. The details of this calculation are given in the *Finite Alpha Range* section. The details of the burn physics are given in the *Burn Physics* section. The details of the coupling between the electrons and radiation are given in the *Radiation* section.

The energy equations of the model are

$$\frac{\partial E_i}{\partial t} = P_{fus}^i - P_{ie} - P_{cond}^i \quad (7)$$

$$\frac{\partial E_e}{\partial t} = P_{fus}^e + P_{ie} - P_{rad} - P_{cond}^e \quad (8)$$

The energy densities of the ion and electron fluids are E_i and E_e , respectively. Units of $\frac{[KeV]}{cm^3}$ are used. The terms on the right hand side of the energy equations are source terms. The total energy sources for the ions and electrons due to the fusion process are P_{fus}^i and P_{fus}^e . The ion-electron energy exchange is defined above in eq.(4). The power loss due to conduction is given by the terms P_{cond} . An expression for P_{cond}^e can be written assuming a gradient scale length for T_e of order R at any given time.

$$P_{cond}^e = \frac{A}{V} \kappa_e \frac{T_e}{R} = \frac{3}{R^2} \kappa_e T_e \quad (9)$$

where A and V are the surface area and volume of the burning fuel sphere. The ion conduction coefficient becomes important to include at ion temperatures in the hundreds of KeV. It is included in this ICF model, and similarly given by

$$P_{cond}^i = \frac{A}{V} \kappa_i \frac{T_i}{R} = \frac{3}{R^2} \kappa_i T_i \quad (10)$$

$$\kappa_i = n_i \kappa_i = 3.9 \frac{3}{4\sqrt{\pi}} \frac{c}{r_e^2 Z_{eff}^2 \ln \Lambda_i} \left(\frac{m_{eff}}{m_e} \right)^2 \left(\frac{T_i}{m_{eff} c^2} \right)^{5/2} \quad (11)$$

The effective mass m_{eff} is defined as $\frac{\rho}{n_i} = \frac{\sum_j m_j n_j}{\sum_j n_j}$ where j is a sum over all thermal ion species (deuterons, tritons, and alphas). The equations governing the densities of the thermal ion popula-

tions are

$$\frac{\partial n_D}{\partial t} = S_D \quad (12)$$

$$\frac{\partial n_T}{\partial t} = S_T \quad (13)$$

$$\frac{\partial n_\alpha}{\partial t} = S_\alpha \quad (14)$$

The number densities n have units of particles/cc. The source terms S_D , S_T , and S_α are determined by the fusion process. Expressions for these terms will be derived in the *Burn Physics* section. In particular, the source term S_α depends on the finite alpha range treatment, which will be discussed below. The equations governing the total particle numbers of the ion populations are

$$\frac{\partial N_D}{\partial t} = V(t) S_D(t) \quad (15)$$

$$\frac{\partial N_T}{\partial t} = V(t) S_T(t) \quad (16)$$

$$\frac{\partial N_\alpha}{\partial t} = V(t) S_\alpha(t) \quad (17)$$

where the volume of the burning fuel sphere is

$$V(t) = \frac{4\pi}{3} R^3(t) \quad (18)$$

$$\frac{\partial R}{\partial t} = -v_r(t) \quad (19)$$

and $R(t)$ is the radius of the incoming rarefaction wave, which moves with velocity $v_r(t)$. The total particle numbers N_j give the total number of particles at a given time in the whole system, including the rarefacted material. Using these total numbers N_j , the total number of fusion reactions that take place within the fuel sphere before its volume shrinks to zero can be determined.

The speed of the rarefaction wave is clearly important. It is well known from MHD theory that the pressure in a plasma fluid equation is the sum of the ion and electron pressures (Francis F. Chen, *Introduction to Plasma Physics and Controlled Fusion* (New York, NY: Springer, 2006) 2006). If

the electron inertia is small compared to the ion inertia, which is typically the case in quasi-neutral plasmas, then the MHD equation of motion is essentially the ion equation of motion. The only hydrodynamic influence the electrons have on the ions is through the electric field, and the only difference between the equations of motion for a normal fluid and a plasma fluid (whose inertia is determined by the ion mass density) is that the plasma fluid has an effective pressure $P_{eff} = P_i + P_e$. In an ideal fluid, a rarefaction wave moves at the sound speed. This is given by

$$v^2 = \frac{dP}{d\rho} = \gamma \frac{P}{\rho} \quad (20)$$

Also, the pressure is defined by $P = nT$. For a small disturbance propagating through an isothermal medium, the temperature is constant and one finds

$$\frac{P}{n} = const \quad (21)$$

Therefore the isothermal assumption is like having a $\gamma = 1$ gas. The sound speed is $v = \sqrt{\frac{P}{\rho}}$. Finally, the rarefaction wave proceeds inwards into the fuel sphere at a speed

$$v_r(t) = \sqrt{\frac{P_i(t) + P_e(t)}{\rho(t)}} \quad (22)$$

3 Burn Physics

The physics of DT burn is central to any ICF code. Indeed, it is the DT fusion reaction on which the entire ICF concept is based. Burn determines the rate at which fuel particles are destroyed, as well as the amount of thermal energy they take with them. Burn also determines the sources of high energy alpha particles and neutrons. Once these fast particles are created, they slow down due to coulomb and nuclear collisions. The process of fast alpha slowing down is described in the *Finite Alpha Range* section. The isothermal model of this thesis concerns a homogenous

medium within an incoming rarefaction wave. The burn physics is simplified in this respect, with a homogeneously isotropic burning region with isotropic fast alpha and neutron production.

In almost all codes, the deuteron and triton populations are assumed to be Maxwellian. In this case the reactivity comes from integrating a Maxwellian distribution over the DT cross section. Much work has been done towards obtaining accurate fits for the DT cross sections, as well as fits for the Maxwellian integrated reactivity. Some codes take into account the enhanced reactivity due to charged particles slowing down from energies much higher than $\frac{3}{2}T_i$. These high energy particles are usually fusion products born at high energy, but can also be thermal particles which get knocked to high energy by 14 MeV neutrons or other fast charged particles through nuclear collisions. These so called knock-ons can have a significant probability of reacting before slowing down if the cross sections are large at the corresponding high center of mass energy. However, neutron heating, knock-ons, and reactions in flight are ignored in this model.

An important effect is the thermal energy which is lost from the thermal ion distribution and which is added to the energy of the fusion products when two particles fuse. If the ion energies are around 200 KeV or higher, this can be an important effect. First the Maxwellian averaged reactivity will be derived, followed by the average thermal energy loss from the ion distribution. Finally, the kinetic fusion source term for the alpha particles will be derived and then used to find the average energy with which alpha particles are born.

3.1 Reactivity

The reactivity is given by

$$\langle \sigma v \rangle = \frac{\int d^3v_1 d^3v_2 \sigma(|\mathbf{v}_1 - \mathbf{v}_2|) |\mathbf{v}_1 - \mathbf{v}_2| f_1(\mathbf{v}_1) f_2(\mathbf{v}_2)}{\int d^3v_1 d^3v_2 f(\mathbf{v}_1) f(\mathbf{v}_2)} \quad (23)$$

where f_1 and f_2 are the distribution functions for the deuterons and tritons. A change of variables can be made

$$\mathbf{v}_1 = \mathbf{v}_c + \mathbf{v} \frac{m_2}{m_1 + m_2} \quad (24)$$

$$\mathbf{v}_2 = \mathbf{v}_c - \mathbf{v} \frac{m_1}{m_1 + m_2} \quad (25)$$

$$d^3 v_1 d^3 v_2 = d^3 v_c d^3 v \quad (26)$$

$$\langle \sigma v \rangle = \frac{1}{n_1 n_2} \int d^3 v_c d^3 v \sigma(v) v f_1\left(\mathbf{v}_c + \mathbf{v} \frac{m_2}{m_1 + m_2}\right) f_2\left(\mathbf{v}_c - \mathbf{v} \frac{m_1}{m_1 + m_2}\right) \quad (27)$$

If both distributions are assumed to be Maxwellian at temperature T , this becomes

$$\langle \sigma v \rangle = \frac{(m_1 m_2)^{3/2}}{(2\pi T)^3} \int d^3 v_c d^3 v \sigma(v) v \exp\left(-\frac{m_1}{2T} \left|\mathbf{v}_c + \mathbf{v} \frac{m_2}{m_1 + m_2}\right|^2 - \frac{m_2}{2T} \left|\mathbf{v}_c - \mathbf{v} \frac{m_1}{m_1 + m_2}\right|^2\right) \quad (28)$$

$$\langle \sigma v \rangle = \frac{(m_1 m_2)^{3/2}}{(2\pi T)^3} \int d^3 v_c d^3 v \sigma(v) v \exp\left(-\frac{m_1 + m_2}{2T} |\mathbf{v}_c|^2 - \frac{1}{2T} \frac{m_1 m_2}{m_1 + m_2} |\mathbf{v}|^2\right) \quad (29)$$

where the cross terms have cancelled. The integral over the center of mass velocity is immediate giving

$$\langle \sigma v \rangle = \frac{(m_1 m_2)^{3/2}}{(2\pi T)^3} \frac{(2\pi T)^{3/2}}{(m_1 + m_2)^{3/2}} \int d^3 v \sigma(v) v \exp\left(-\frac{1}{2T} \frac{m_1 m_2}{m_1 + m_2} |\mathbf{v}|^2\right) \quad (30)$$

$$\langle \sigma v \rangle = \left(\frac{\mu}{2\pi T}\right)^{3/2} \int d^3 v \sigma(v) v \exp\left(-\frac{1}{2T} \mu v^2\right) \quad (31)$$

Converting to spherical coordinates, performing the angular integration, and finally converting to center of mass energy $\varepsilon = 1/2 \mu v^2$, gives the reactivity

$$\langle \sigma v \rangle = 4\pi \left(\frac{\mu}{2\pi T}\right)^{3/2} \int dv \sigma(v) v^3 \exp\left(-\frac{1}{2T} \mu v^2\right) \quad (32)$$

$$\langle \sigma v \rangle = \sqrt{\frac{2}{\pi \mu c^2}} \frac{2c}{T^{3/2}} \int d\varepsilon \sigma(\varepsilon) \varepsilon \exp\left(-\frac{\varepsilon}{T}\right) \quad (33)$$

3.2 Rate of Energy Loss From Thermal Distribution Due to Fusion

The average rate of energy loss per unit volume from the thermal ion distribution is given by

$$P_{loss} = \int d^3 v_1 d^3 v_2 \sigma(|\mathbf{v}_1 - \mathbf{v}_2|) |\mathbf{v}_1 - \mathbf{v}_2| \left(\frac{1}{2} m_1 v_1^2 + \frac{1}{2} m_2 v_2^2\right) f_1(\mathbf{v}_1) f_2(\mathbf{v}_2) \quad (34)$$

Each fusion reaction, with incident particles having velocities v_1 and v_2 , removes one thermal ion with energy $\frac{1}{2}m_1v_1^2$ and another with energy $\frac{1}{2}m_2v_2^2$. This energy is distributed among the fusion products in addition to the mass-energy released by the fusion reaction. Performing the change of variables as was done above gives

$$P_{loss} = \int d^3v_c d^3v \sigma(v) v \left(\frac{1}{2}m_1 \left| \mathbf{v}_c + \mathbf{v} \frac{m_2}{m_1 + m_2} \right|^2 + \frac{1}{2}m_2 \left| \mathbf{v}_c - \mathbf{v} \frac{m_1}{m_1 + m_2} \right|^2 \right) \quad (35)$$

$$\cdot f_1\left(\mathbf{v}_c + \mathbf{v} \frac{m_2}{m_1 + m_2}\right) f_2\left(\mathbf{v}_c - \mathbf{v} \frac{m_1}{m_1 + m_2}\right) \quad (36)$$

$$P_{loss} = n_1 n_2 \frac{(m_1 m_2)^{3/2}}{(2\pi T)^3} \int d^3v_c d^3v \sigma(v) v \left(\frac{m_1 + m_2}{2} |\mathbf{v}_c|^2 + \frac{1}{2} \frac{m_1 m_2}{m_1 + m_2} |\mathbf{v}|^2 \right) \quad (37)$$

$$\cdot \exp\left(-\frac{m_1 + m_2}{2T} |\mathbf{v}_c|^2 - \frac{1}{2T} \frac{m_1 m_2}{m_1 + m_2} |\mathbf{v}|^2\right) \quad (38)$$

$$P_{loss} = n_1 n_2 \frac{(m_1 m_2)^{3/2}}{2 (2\pi T)^3} (4\pi)^2 \int dv_c dv \sigma(v) v_c^2 v^3 (M v_c^2 + \mu v^2) \exp\left(-\frac{1}{2T} M v_c^2 - \frac{1}{2T} \mu v^2\right) \quad (39)$$

It is convenient to break this expression up into two integrals, $P_{loss} = I_\varepsilon + I_{CM}$. The first is an integral over the relative energy ε

$$I_\varepsilon = n_1 n_2 \mu^{5/2} \frac{(2\pi T)^{3/2}}{4\pi^2 T^3} \int dv \sigma(v) v^5 \exp\left(-\frac{1}{2T} \mu v^2\right) \quad (40)$$

$$I_\varepsilon = n_1 n_2 \sqrt{\frac{2}{\pi \mu c^2}} \frac{2c}{T^{3/2}} \int d\varepsilon \sigma(\varepsilon) \varepsilon^2 \exp\left(-\frac{\varepsilon}{T}\right) \quad (41)$$

The second is an integral over the center of mass energy

$$I_{CM} = n_1 n_2 M \frac{(m_1 m_2)^{3/2}}{2 (2\pi T)^3} (4\pi)^2 \int dv_c dv \sigma(v) v_c^4 v^3 \exp\left(-\frac{1}{2T} M v_c^2 - \frac{1}{2T} \mu v^2\right) \quad (42)$$

$$I_{CM} = \frac{3}{2} T n_1 n_2 \sqrt{\frac{2}{\pi \mu c^2}} \frac{2c}{T^{3/2}} \int d\varepsilon \sigma(\varepsilon) \varepsilon \exp\left(-\frac{\varepsilon}{T}\right) = \frac{3}{2} T n_1 n_2 \langle \sigma v \rangle \quad (43)$$

This finally gives

$$P_{loss} = n_1 n_2 \left(\frac{3}{2} T \langle \sigma v \rangle + \langle \sigma v \varepsilon \rangle \right) \quad (44)$$

$$\langle \sigma v \rangle = \sqrt{\frac{2}{\pi \mu c^2}} \frac{2c}{T^{3/2}} \int d\varepsilon \sigma(\varepsilon) \varepsilon \exp\left(-\frac{\varepsilon}{T}\right) \quad (45)$$

$$\langle \sigma v \varepsilon \rangle = \sqrt{\frac{2}{\pi \mu c^2}} \frac{2c}{T^{3/2}} \int d\varepsilon \sigma(\varepsilon) \varepsilon^2 \exp\left(-\frac{\varepsilon}{T}\right) \quad (46)$$

For the cross section, the Bosch-Hale fit for DT is used (H.S. Bosch & G.M. Hale, *Nucl. Fusion*, vol. 32, 611 (1992) 1992). It is given by

$$\sigma(\varepsilon) = \frac{s(\varepsilon)}{\varepsilon} \exp\left(-\sqrt{\frac{E_g}{\varepsilon}}\right) \quad [\text{bn}] \quad (47)$$

$$s(\varepsilon) = \frac{A_1 + \varepsilon(A_2 + \varepsilon(A_3 + \varepsilon(A_4 + \varepsilon A_5)))}{1 + \varepsilon(B_1 + \varepsilon(B_2 + \varepsilon(B_3 + \varepsilon B_4)))} \quad (48)$$

$$A_1 = 6.927 \times 10^1 \quad (49)$$

$$A_2 = 7.454 \times 10^5 \quad (50)$$

$$A_3 = 2.050 \times 10^3 \quad (51)$$

$$A_4 = 5.2002 \times 10^1 \quad (52)$$

$$A_5 = 0 \quad (53)$$

$$B_1 = 6.38 \times 10^1 \quad (54)$$

$$B_2 = -9.95 \times 10^{-1} \quad (55)$$

$$B_3 = 6.981 \times 10^{-5} \quad (56)$$

$$B_4 = 1.728 \times 10^{-4} \quad (57)$$

$$E_g = 1182.2 \quad (58)$$

Here the quantities $\langle\sigma v\rangle$ and $\langle\sigma v\varepsilon\rangle$ are functions of ion temperature only. During burn, a loss term given by P_{loss} above should be included in the ion energy equation. Furthermore, the average of the sum of the charged particle product energies for a single fusion reaction becomes

$$Q + \frac{3}{2}T_i + \frac{\langle\sigma v\varepsilon\rangle}{\langle\sigma v\rangle} \quad (59)$$

The first term is the DT reaction Q value, $Q = 17590$ KeV. The second two terms constitute the average energy which two particles have when they do fuse and are removed from the thermal populations. For $T_i = 200$ keV, the second two terms sum to 496 keV and for $T_i = 300$ they sum to 721 keV. Finally, this energy is distributed among the two product particles: a neutron and an alpha particle. The average energy that the two fusion product particles receive must be calculated from the initial particle distribution functions and the fusion cross section.

Consider a fusion reaction where the product particles, labeled 3 and 4, have masses m_3 and m_4 . It is expected that the reaction energy Q and initial relative energy $\frac{\langle\sigma v\varepsilon\rangle}{\langle\sigma v\rangle}$ are distributed by the opposite mass ratio, for example, the fraction of this energy given to particle 3 is $\frac{m_4}{m_3+m_4}$. This can be derived from elementary kinetic considerations in the center of mass frame where the total momentum is zero. It is expected that the center of mass energy $\frac{3}{2}T_i$ is split in proportion to the particle masses, for example, the fraction of this CM energy given to particle 3 is $\frac{m_3}{m_3+m_4}$. Therefore, the initial energy of a neutron and an alpha particles on average is

$$E_{no} = \left(Q + \frac{\langle\sigma v\varepsilon\rangle}{\langle\sigma v\rangle} \right) \frac{m_\alpha}{m_\alpha + m_n} + \frac{3}{2}T_i \frac{m_n}{m_\alpha + m_n} \quad (60)$$

$$E_{\alpha o} = \left(Q + \frac{\langle\sigma v\varepsilon\rangle}{\langle\sigma v\rangle} \right) \frac{m_n}{m_\alpha + m_n} + \frac{3}{2}T_i \frac{m_\alpha}{m_\alpha + m_n} \quad (61)$$

In order to prove this, the kinetic source term for product fusion particles will be calculated under the assumption that the Q value is large compared to the average center of mass energy. The energy moment of this source term will result in the first term in the above equations. Furthermore, the isothermal model assumes all alpha particles are born at their average energy. This is strictly not correct, as there is a distribution about this average energy. Upon calculation of the kinetic source

term, the width of this distribution can be determined.

3.3 Distribution of Fusion Products

Consider two particles of mass m_1 and m_2 fusing and producing two particles of mass m_3 and m_4 . Assume that the fluid velocity is small compared to the average thermal velocity so that the lab frame and the fluid frame can be considered the same. Let \vec{P} be the total momentum in the *fluid* frame, and E be the total energy, including mass-energy Q released due to fusion. To a good approximation, conservation of mass still holds, $m_1 + m_2 = m_3 + m_4 = M$. Conservation of energy and momentum gives

$$m_1\vec{v}_1 + m_2\vec{v}_2 = \vec{P} = m_3\vec{v}_3 + m_4\vec{v}_4 \quad (62)$$

$$m_1v_1^2 + m_2v_2^2 + 2Q = 2E = m_3v_3^2 + m_4v_4^2 \quad (63)$$

A constraint on \vec{v}_3 , taking \vec{P} and E as given, can be found from these two equations

$$\left| \vec{P} - m_3\vec{v}_3 \right|^2 = m_4^2v_4^2 = 2m_4E - m_4m_3v_3^2 \quad (64)$$

$$v_3^2 - \frac{2\vec{P} \cdot \vec{v}_3}{M} + \frac{P^2 - 2m_4E}{m_3M} = 0 \quad (65)$$

If \vec{v}_3 is considered fixed, then the above equation can be considered a constraint on the velocities \vec{v}_1 and \vec{v}_2 . The number of fusion reactions occurring per volume per second within $dv_1^3 dv_2^3$ (ie, given a specific \vec{v}_1 and \vec{v}_2) is given by

$$d^3v_1 d^3v_2 \sigma (|\mathbf{v}_1 - \mathbf{v}_2|) |\mathbf{v}_1 - \mathbf{v}_2| f_1(\mathbf{v}_1) f_2(\mathbf{v}_2) \quad (66)$$

Therefore, the number of fusion product particles with mass m_3 , produced per unit volume per second within dv_3^3 with a velocity \vec{v}_3 in the fluid frame is

$$S_3(\vec{v}_3) = \int_C d^3v_1 d^3v_2 \sigma (|\mathbf{v}_1 - \mathbf{v}_2|) |\mathbf{v}_1 - \mathbf{v}_2| f_1(\mathbf{v}_1) f_2(\mathbf{v}_2) \quad (67)$$

where C implies that the integration is subject to the constraint eq.(65) for \vec{v}_1 and \vec{v}_2 .

Converting to center of mass coordinates

$$\mathbf{v}_1 = \mathbf{v}_c + \mathbf{v} \frac{m_2}{m_1 + m_2} \quad (68)$$

$$\mathbf{v}_2 = \mathbf{v}_c - \mathbf{v} \frac{m_1}{m_1 + m_2} \quad (69)$$

$$d^3 v_1 d^3 v_2 = d^3 v_c d^3 v \quad (70)$$

results in

$$S_3(\vec{v}_3) = \int_C d^3 v_c d^3 v \sigma(v) v f(\mathbf{v}_c) f(\mathbf{v}) \quad (71)$$

$$v_3^2 - 2\vec{v}_c \cdot \vec{v}_3 + v_c^2 - \frac{m_4}{m_3} \frac{2Q + \mu v^2}{M} = 0 \quad (72)$$

where μ is the reduced mass. The constraint restricts the volume integral over $d\vec{v}_c$ to an integration over a spherical surface in \vec{v}_c space, such that the difference between the fixed vector \vec{v}_3 and \vec{v}_c always has magnitude $K \equiv \sqrt{\frac{m_4}{m_3} \frac{2Q + \mu v^2}{M}}$. Let the vector \vec{v}_3 lies along the z axis in \vec{v}_c space. The integral is easiest to do in terms of a coordinate system whose origin is at the center of the spherical surface constraint. The geometry and this surface are shown in figure (1).

The result is, noting that everything depends only on the magnitudes of v_3 and v ,

$$S_3(v_3) = \frac{1}{2} \int_0^\pi \sin \alpha d\alpha d^3 v \sigma(v) v f(v_c[\alpha, v]) f(v) \quad (73)$$

$$v_c^2[\alpha, v] = v_3^2 + \frac{m_4}{m_3} \frac{2Q + \mu v^2}{M} + 2v_3 \sqrt{\frac{m_4}{m_3} \frac{2Q + \mu v^2}{M}} \cos \alpha \quad (74)$$

Plugging in Maxwellian distributions gives

$$S_3(v_3) = \int_{-1}^1 d\mu \exp \left(-\frac{M}{2T} \left[v_3^2 + \frac{m_4}{m_3} \frac{2Q + \mu v^2}{M} + 2v_3 \sqrt{\frac{m_4}{m_3} \frac{2Q + \mu v^2}{M}} \mu \right] \right) \quad (75)$$

$$\cdot \frac{n_1 n_2 (m_1 m_2)^{3/2}}{2 (2\pi T)^3} \int d^3 v \sigma(v) v \exp \left(-\frac{\mu}{2T} v^2 \right) \quad (76)$$

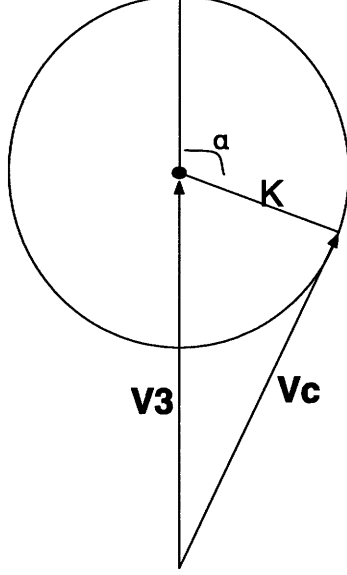


Figure 1: Geometry for calculating fusion particle source distribution.

Just focusing on the first term

$$\int_{-1}^1 d\mu \exp \left(-\frac{M}{2T} \left[v_3^2 + \frac{m_4}{m_3} \frac{2Q + \mu v^2}{M} + 2v_3 \sqrt{\frac{m_4}{m_3} \frac{2Q + \mu v^2}{M}} \mu \right] \right) \quad (77)$$

$$= \exp \left(-\frac{M}{2T} v_3^2 \right) \exp \left(-\frac{M}{2T} \frac{m_4}{m_3} \frac{2Q + \mu v^2}{M} \right) \int_{-1}^1 d\mu \exp \left(-\frac{v_3 M}{T} \sqrt{\frac{m_4}{m_3} \frac{2Q + \mu v^2}{M}} \mu \right) \quad (78)$$

note that the μ in front of the relative velocity is the reduced mass, where the other μ 's are the angle cosines. The integral is

$$\int_{-1}^1 d\mu \exp \left(-\frac{v_3 M}{T} \sqrt{\frac{m_4}{m_3} \frac{2Q + \mu v^2}{M}} \mu \right) = \frac{2T}{v_3 M} \sqrt{\frac{m_3}{m_4} \frac{M}{2Q + \mu v^2}} \sinh \left(\frac{v_3 M}{T} \sqrt{\frac{m_4}{m_3} \frac{2Q + \mu v^2}{M}} \right) \quad (79)$$

Putting everything together:

$$S_3(v_3) = n_1 n_2 \frac{(m_1 m_2)^{3/2}}{(2\pi T)^3} \frac{T}{M v_3} \exp\left(-\frac{M}{2T} v_3^2\right) \quad (80)$$

$$\cdot \int d^3 v \sigma(v) v \exp\left(-\frac{M}{2T} \frac{m_4}{m_3} \frac{2Q + \mu v^2}{M}\right) \sqrt{\frac{m_3}{m_4} \frac{M}{2Q + \mu v^2}} \quad (81)$$

$$\cdot \sinh\left(\frac{v_3 M}{T} \sqrt{\frac{m_4}{m_3} \frac{2Q + \mu v^2}{M}}\right) \exp\left(-\frac{\mu}{2T} v^2\right) \quad (82)$$

This expression is exact. However, it is complicated. To proceed, the limit $2Q \gg \mu v^2$ is taken.

This assumes that the energy released in the fusion reaction is much greater than the energy of the two thermal particles in their center of mass frame before fusion. This may not always be the case.

Furthermore, the assumption that $2Q \gg M v_c^2$ is never made. Continuing with $2Q \gg \mu v^2$

$$S_3(v_3) = n_1 n_2 \frac{(m_1 m_2)^{3/2}}{(2\pi T)^3} \frac{T}{v_3 M} \sqrt{\frac{m_3}{m_4} \frac{M}{2Q}} \quad (83)$$

$$\cdot \exp\left(-\frac{M}{2T} v_3^2\right) \sinh\left(\frac{v_3 M}{T} \sqrt{\frac{m_4}{m_3} \frac{2Q}{M}}\right) \exp\left(-\frac{M}{2T} \frac{m_4}{m_3} \frac{2Q}{M}\right) \quad (84)$$

$$\cdot \int d^3 v \sigma(v) v \exp\left(-\frac{\mu}{2T} v^2\right) \quad (85)$$

where now the integral over the relative velocity is the same as that which gives the reactivity $\langle \sigma v \rangle$.

If the assumption $2Q \gg \mu v^2$ is made, it is also a good approximation to assume $Q \gg T$, and

since v_3 is the velocity of a fusion product, the approximation $\frac{v_3}{T} \frac{m_4}{m_3} 2Q \gg 1$ is good. Therefore, the hyperbolic sine function just becomes a positive exponential. This results in a simpler expression

$$S_3(v_3) = n_1 n_2 \frac{(m_1 m_2)^{3/2}}{(2\pi T)^3} \frac{T}{2v_3 M} \sqrt{\frac{m_3}{m_4} \frac{M}{2Q}} \quad (86)$$

$$\cdot \exp\left(-\frac{M}{2T} \left(v_3 - \sqrt{\frac{m_4}{m_3} \frac{2Q}{M}}\right)^2\right) \int d^3 v \sigma(v) v \exp\left(-\frac{\mu}{2T} v^2\right) \quad (87)$$

Noting that

$$\langle \sigma v \rangle = \left(\frac{\mu}{2\pi T} \right)^{3/2} \int d^3 v \sigma(v) v \exp\left(-\frac{1}{2T} \mu v^2\right) \quad (88)$$

The expression can be written

$$S_3(v_3) = n_1 n_2 \frac{(m_1 m_2)^{3/2}}{(2\pi T)^3} \frac{T}{2v_3 M} \sqrt{\frac{m_3 M}{m_4 2Q}} \exp\left(-\frac{M}{2T} \left(v_3 - \sqrt{\frac{m_4 2Q}{m_3 M}}\right)^2\right) \langle \sigma v \rangle \left(\frac{2\pi T}{\mu}\right)^{3/2} \quad (89)$$

$$S_3(v_3) = \left(\frac{M}{2\pi T}\right)^{3/2} \frac{T}{2v_3 M} \sqrt{\frac{m_3 M}{m_4 2Q}} \exp\left(-\frac{M}{2T} \left(v_3 - \sqrt{\frac{m_4 2Q}{m_3 M}}\right)^2\right) \langle \sigma v \rangle n_1 n_2 \quad (90)$$

The total number of m_3 particles produced per second is given by the first moment of the kinetic source term, and this is expected to be

$$\int dv_3^3 S_3(v_3) = \langle \sigma v \rangle n_1 n_2 \quad (91)$$

Given the assumption that $Q \gg T$, it is expected that

$$1 = 4\pi \left(\frac{M}{2\pi T}\right)^{3/2} \frac{T}{2M} \sqrt{\frac{m_3 M}{m_4 2Q}} \int dv_3 v_3 \exp\left(-\frac{M}{2T} \left(v_3 - \sqrt{\frac{m_4 2Q}{m_3 M}}\right)^2\right) \quad (92)$$

and upon performing the integral, one finds that the distribution is properly normalized. Therefore in the limit $Q \ll T \approx \mu v^2$, the source term for particles of mass m_3 is

$$S_3(v_3) = \left(\frac{M}{2\pi T}\right)^{3/2} \sqrt{\frac{m_3 M}{m_4 2Q}} \frac{T}{2M v_3} \exp\left(-\frac{M}{2T} \left(v_3 - \sqrt{\frac{m_4 2Q}{m_3 M}}\right)^2\right) \langle \sigma v \rangle n_1 n_2 \quad (93)$$

The normalized source distribution of alpha particles, $\int dv_\alpha^3 S_\alpha = \langle \sigma v \rangle n_1 n_2$, is

$$S_\alpha(v_\alpha) = \frac{m_n + m_\alpha}{8\pi^{3/2}} \sqrt{\frac{m_\alpha}{m_n Q T}} \frac{1}{v_\alpha} \exp\left(-\frac{m_n + m_\alpha}{2T} \left(v_\alpha - \sqrt{\frac{m_n 2Q}{m_\alpha m_n + m_\alpha}}\right)^2\right) \langle \sigma v \rangle n_1 n_2 \quad (94)$$

The average energy, taking the limit $Q \ll T \approx \mu v^2$, is found to be precisely

$$4\pi \int dv_3 v_3^2 \frac{1}{2} m_3 v_3^2 f_3 = \frac{m_4 Q}{m_4 + m_3} + \frac{m_3}{m_4 + m_3} \frac{3}{2} T \quad (95)$$

which is as expected. The center of mass energy, which does not appear here due to the assumptions above that $2Q \gg \mu v^2$, would be added to the reaction energy Q . This is true on the average because it is true for every single specific reaction for a given \vec{v}_1 and \vec{v}_2 . The final result for the average energy with which an alpha particle is born is given by

$$\langle E_\alpha \rangle = \frac{m_n}{m_\alpha + m_n} \left(Q + \frac{\langle \sigma v \varepsilon \rangle}{\langle \sigma v \rangle} \right) + \frac{m_\alpha}{m_\alpha + m_n} \frac{3}{2} T \quad (96)$$

This initial alpha particle energy $\langle E_\alpha \rangle$ is used in the finite alpha range model to determine the slowing down dynamics. This energy effects the alpha particle's range as well as the amount of energy that gets transferred to the electrons and ions. Now, loss terms due to fusion can be included in eqs.(7).

$$\frac{\partial E_i}{\partial t} = P_{fus}^i - n_D n_T \left(\frac{3}{2} T_i \langle \sigma v \rangle + \langle \sigma v \varepsilon \rangle \right) - P_{ie} - P_{cond}^i \quad (97)$$

$$\frac{\partial E_e}{\partial t} = P_{fus}^e + P_{ie} - P_{rad} - P_{cond}^e \quad (98)$$

$$\frac{\partial n_D}{\partial t} = -n_D n_T \langle \sigma v \rangle \quad (99)$$

$$\frac{\partial n_T}{\partial t} = -n_D n_T \langle \sigma v \rangle \quad (100)$$

$$\frac{\partial n_\alpha}{\partial t} = S_\alpha \quad (101)$$

where P_{fus}^i and P_{fus}^e correspond to only *heating* terms due to the energy transfer from fast alpha particles. They are determined from R , E_α , and the details of the slowing down model. The alpha source term S_α is determined from the slowing down model as well.

4 Finite Alpha Range

Fast alpha particles slow down through coulomb collisions with the thermal ion and electron populations. This typically happens on a fast time scale compared to the fusion rate, as will be shown below. Therefore it is assumed that when an alpha particle is born, it slows down and transfers its energy before any of the macroscopic variables change significantly, ie, alphas slow down in a fixed homogenous background with fixed temperatures and densities. Of course, once an alpha reaches the spherical shell of the rarefaction wave, it is assumed lost and no longer gives its energy to the homogenous fuel sphere.

The fast alpha particles transfer part of their initial energy to the electrons and part to the ions. The fractional splitting is primarily determined by the electron temperature. The electrons are preferentially heated at low T_e ($T_e < \approx 25$), while it is the ions that are preferentially heated at larger T_e ($T_e > \approx 25$). The ion temperature determines the fusion reactivity, and the ions are coupled to the electrons which have roughly the same heat capacity. Also, the electrons couple to the radiation which can be a large heat sink. The fractional energy splitting is clearly important and effects the whole burn process. Many codes use simple formulae for this fractional splitting, such as the well known Fraley (Fraley *et al.* 1974) empirical result $f_i = \frac{1}{1+32/T_e}$, where f_i is the fraction of fusion energy given to the ions by the fast alpha particles. However, these simple formulas can lead to significant errors in the burn dynamics. The fractional splitting is not just determined by the electron temperature but by Z_{eff} , both electron and ion coulomb logarithms, and even the ion temperature although with somewhat weak dependence.

In this section, an equation governing the slowing down of a fast alpha particle in a background ion-electron plasma will be derived from the Fokker Plank equation. Upon taking appropriate limits of the Chandrasekhar function, an analytic expression for the range of an alpha particle including ion collisions will be derived. Furthermore, the functional form of the Fraley splitting formula can be found from an asymptotic expansion, resulting in an expression for the numerical factor. This expression will be compared with numerical results from integrating the slowing down rate equation. In terms of the ICF burn code, the slowing down equation for the alpha particles will be

numerically integrated at every time step. The details of this will be discussed below. Finally, an expression for the total energy and number of alpha particles deposited in the finite fuel sphere at any given time will be derived.

4.1 Slowing Down Equation

The initial assumptions concerning the slowing down of a fast particle are as follows. Fast charged particles in a background of ions and electrons tend to move in a straight line until their energy becomes comparable to the ion thermal energy. At this point the deflection frequency becomes large. Although the homogenous assumption leads to charged particles being isotropically produced, any given fast charged particle moves on a straight line as if it were emitted from a source distribution function given by

$$f_\alpha(\mathbf{v}) = n_\alpha \delta(\mathbf{v} - \mathbf{u}_\alpha) \quad (102)$$

Of course, this assumption does not deal with the deflection of the charged particles near the end of their range due to collisions with ions, and it is assumed here that every alpha particle, while emitted isotropically, follows the average behavior of particles given by the source eq.(102). This is a shortcoming of the current treatment which ignores particle diffusion.

The Fokker Plank equation in cartesian coordinates is

$$\frac{\partial f_T}{\partial t} = L^{TF} \left[\frac{\partial}{\partial \mathbf{v}} \frac{\partial}{\partial \mathbf{v}} : \left(f_T \frac{\partial^2}{\partial \mathbf{v} \partial \mathbf{v}} \psi_F \right) - \frac{m_T}{\mu} \frac{\partial}{\partial \mathbf{v}} \cdot \left(f_T \frac{\partial \varphi_F}{\partial \mathbf{v}} \right) \right] \quad (103)$$

$$L^{TF} = \left(\frac{z_T z_F e^2}{\epsilon_o m_T} \right)^2 \ln(\Lambda_F) \quad \epsilon_o \Rightarrow \frac{1}{4\pi} \text{ for cgs} \quad (104)$$

The T subscript stands for test particle and the F subscript stands for field particle. The test particles here are the fast alphas and the field particles consist of thermal ions and electrons. The

Rosenbluth potentials ψ_F and φ_F are given by

$$\psi_F = \frac{1}{8\pi} \int u f_F(\mathbf{v}') d\mathbf{v}' \quad (105)$$

$$\varphi_F = \frac{1}{4\pi} \int \frac{f_F(\mathbf{v}')}{u} d\mathbf{v}' \quad (106)$$

$$u = |\mathbf{v} - \mathbf{v}'| \quad (107)$$

The mean velocity of fast alpha particles with distribution f_α is

$$\mathbf{u}_\alpha = \frac{1}{n_\alpha} \int \mathbf{v} f_\alpha d^3\mathbf{v} \quad (108)$$

The rate of change of this mean velocity assuming the initial alpha distribution eq.(102) is

$$\frac{\partial \mathbf{u}_\alpha}{\partial t} = \int d^3\mathbf{v} \mathbf{v} \frac{L^{TF}}{n_\alpha} \left[\frac{\partial}{\partial \mathbf{v}} \frac{\partial}{\partial \mathbf{v}} : \left(f_\alpha \frac{\partial^2}{\partial \mathbf{v} \partial \mathbf{v}} \psi_F \right) - \frac{m_\alpha}{\mu} \frac{\partial}{\partial \mathbf{v}} \cdot \left(f_\alpha \frac{\partial \varphi_F}{\partial \mathbf{v}} \right) \right] \quad (109)$$

Integration by parts on the second term above has the form

$$\int d^3\mathbf{v} v_k \frac{\partial}{\partial v_\beta} J_\beta = \int d^3\mathbf{v} \left(\frac{\partial}{\partial v_\beta} v_k J_\beta - J_\beta \frac{\partial}{\partial v_\beta} v_k \right) \quad (110)$$

$$= \int d^3\mathbf{v} \left(\frac{\partial}{\partial v_\beta} v_k J_\beta - J_\beta \frac{\partial}{\partial v_\beta} v_k \right) = - \int d^3\mathbf{v} J_\beta \delta_{\beta k} = - \int d^3\mathbf{v} J_k \quad (111)$$

$$\Rightarrow - \int d^3\mathbf{v} \mathbf{v} \frac{\partial}{\partial \mathbf{v}} \cdot \left(f_\alpha \frac{\partial \varphi_F}{\partial \mathbf{v}} \right) = \int d^3\mathbf{v} f_\alpha \frac{\partial \varphi_F}{\partial \mathbf{v}} \quad (112)$$

And similarly for the first term

$$\int d^3\mathbf{v} \mathbf{v} \frac{\partial}{\partial \mathbf{v}} \frac{\partial}{\partial \mathbf{v}} : \left(f_\alpha \frac{\partial^2}{\partial \mathbf{v} \partial \mathbf{v}} \psi_F \right) = - \int d^3\mathbf{v} \frac{\partial}{\partial \mathbf{v}} \cdot \left(f_\alpha \frac{\partial^2}{\partial \mathbf{v} \partial \mathbf{v}} \psi_F \right) = 0 \quad (113)$$

It is seen that the term responsible for diffusion gives a zero velocity moment, as expected. As fast alphas slow down, they begin to diffuse and gain a perpendicular velocity component. The average of this component is however zero. The assumption that every alpha particle moves with this mean velocity \mathbf{u}_α is precisely where the diffusion error discussed above enters in. The slowing

down equation is now

$$\frac{\partial \mathbf{u}_\alpha}{\partial t} = \frac{L^{\alpha F} m_\alpha}{n_\alpha \mu} \int d^3 \mathbf{v} f_\alpha \frac{\partial \varphi_F}{\partial \mathbf{v}} \quad (114)$$

Since the alpha distribution is a delta function, the integral is straightforward

$$\frac{\partial \mathbf{u}_\alpha}{\partial t} = \frac{L^{\alpha F} m_\alpha}{n_\alpha \mu} n_\alpha \frac{\partial \varphi_F}{\partial \mathbf{v}} \Big|_{\mathbf{v}=\mathbf{u}_\alpha} = L^{\alpha F} \frac{m_\alpha}{\mu} \left[\frac{\mathbf{v}}{v} \frac{\partial \varphi_F}{\partial v} \right] \Big|_{\mathbf{v}=\mathbf{u}_\alpha} \quad (115)$$

The Rosenbluth potential is spherically symmetric because the field particles are isotropic. It can be shown that the derivative of the Rosenbluth potential (Helander & Sigmar 2002) is

$$\frac{\partial \varphi_F}{\partial v} = -\frac{m_F n_F}{4\pi T_F} G(y) \quad (116)$$

$$y = u_\alpha / v_{Th,F} \quad (117)$$

$$G(y) = \frac{\text{erf}(y) - y \text{erf}'(y)}{2y} \quad (118)$$

where y is the alpha particle velocity normalized to the thermal velocity of the field particles, and $G(y)$ is the Chandrasekhar function. Also, the rate of change of \mathbf{u}_α is in the direction (negative) of \mathbf{u}_α . What results is a scalar equation for the magnitude of the mean alpha velocity

$$\frac{\partial u_\alpha}{\partial t} = -L^{\alpha F} \frac{m_\alpha}{\mu} \frac{n_F}{2\pi v_{Th,F}^2} G(y) = -L^{\alpha F} \frac{m_\alpha}{\mu} \frac{m_F n_F}{4\pi T_F} G(y) \quad (119)$$

$$\frac{\partial \beta_\alpha}{\partial t} = -6 \frac{n_F}{n_e} z_F^2 \nu_T \frac{(m_e c^2)^2}{T_F m_\alpha c^2} \left(1 + \frac{m_F}{m_\alpha} \right) \ln(\Lambda_F) G(y) \quad (120)$$

where β is the alpha velocity normalized to c . The equation has been written so that the Thomson rate is the only quantity that carries units. The field particles F consist of thermal deuterons, tritons, alpha particles, and electrons. Because the Fokker Plank equation is linear, the final expression is just a sum of contributions and is

$$\frac{\partial \beta_\alpha}{\partial t} = -6 \nu_T \frac{m_e}{m_\alpha} \psi_{eff} \ln(\Lambda_i) \frac{m_e c^2}{T_i} G(y_i) - 6 \nu_T \frac{m_e}{m_\alpha} \ln(\Lambda_e) \frac{m_e c^2}{T_e} G(y_e) \quad (121)$$

$$\psi_{eff} = \left(Z_{eff} + \frac{1}{n_e m_\alpha} \sum_j n_j m_j Z_j^2 \right) \quad (122)$$

where the sum is over all of the thermal ion species, y_i and y_e are the alpha velocity u_α normalized to the ion and electron thermal velocity, respectively, and an effective parameter ψ_{eff} is used to simplify the notation. When alpha particles thermalize with the homogenous background plasma and become part of the thermal ion distribution, their mean velocity \mathbf{u}_α is zero, and all of the initial energy of each alpha particle, $\frac{1}{2} m_\alpha u_{\alpha 0}^2$, has been given to the thermal electron and ion distributions. Therefore every alpha particle is born with energy $E_{\alpha 0}$ determined by the burn physics, has an initial velocity $u_{\alpha 0} = \sqrt{\frac{2E_{\alpha 0}}{m_\alpha}}$, and travels in a straight line with its slowing down governed by eq.(121) until its velocity u_α is zero. At this point an alpha particle becomes part of the thermal ion distribution at the end of its range.

The stopping power can also be calculated

$$\frac{\partial E_\alpha}{\partial x} = \frac{1}{u_\alpha} \frac{\partial E_\alpha}{\partial t} = m_\alpha \frac{\partial u_\alpha}{\partial t} \quad (123)$$

$$-\frac{\partial E_\alpha}{\partial x} = 6 \frac{\nu_T}{c} \psi_{eff} \ln(\Lambda_i) \frac{(m_e c^2)^2}{T_i} G(y_i) + 6 \frac{\nu_T}{c} \ln(\Lambda_e) \frac{(m_e c^2)^2}{T_e} G(y_e) \quad (124)$$

where now y_i and y_e are expressed as functions of the alpha particle energy E_α

$$y_i = \sqrt{\frac{m_{eff} E_\alpha}{m_\alpha T_i}} \quad (125)$$

$$y_e = \sqrt{\frac{m_e E_\alpha}{m_\alpha T_e}} \quad (126)$$

It is convenient to re-write the stopping power in terms of dimensionless quantities

$$\bar{E} = \frac{E_\alpha}{m_e c^2} \quad \bar{x} = \frac{\nu_T}{c} x \quad (127)$$

$$-\frac{\partial \bar{E}}{\partial \bar{x}} = 6 \psi_{eff} \ln(\Lambda_i) \frac{m_e c^2}{T_i} G(y_i) + 6 \ln(\Lambda_e) \frac{m_e c^2}{T_e} G(y_e) \quad (128)$$

This is the equation which the burn code numerically integrates at every time step. At any point along the path, the fraction of the energy that instantaneously goes to the ions is given by

$$f_i(\bar{x}) = \frac{\psi_{eff} \ln(\Lambda_i) G(y_i)}{\psi_{eff} \ln(\Lambda_i) G(y_i) + \ln(\Lambda_e) \frac{T_i}{T_e} G(y_e)} \quad (129)$$

Once the energy \bar{E} is integrated to zero along its path, the fraction of the total initial energy $E_{\alpha 0}$ that is given to the ions, f_i , can be found.

4.2 Limits and Approximations

Some very useful formulae can be derived by taking simple approximations of the slowing down equation and stopping power. The Chandrasekhar function has the following limits

$$G(y) \approx \frac{2y}{3\sqrt{\pi}} \quad y \ll 1 \quad (130)$$

$$G(y) \approx \frac{1}{2y^2} \quad y \gg 1 \quad (131)$$

For a good range of an alpha particle's energy, its speed is slower than the electron thermal speed and faster than the ion thermal speed. For $T_e = 30$ KeV, $T_i = 100$ KeV, and an alpha particle that is just born with $E_{\alpha} = 3500$, $y_i = 148$ and $y_e = 4$. As the alpha particle slows down, y_i decreases while y_e increases. Therefore, the ion $G(y_i)$ can take the $y \gg 1$ limit and the electron $G(y_e)$ can take the $y \ll 1$ limit. If these approximations are made, the stopping power eq.(128) can be integrated to give an analytic expression for an alpha particle's range. The slowing down eq.(121) can be integrated to give an analytic expression for an alpha particle's velocity as a function of time. An expression for the stopping time, as well as an expression for the energy splitting fraction, can be derived from this.

Taking the appropriate limits, the stopping power equation becomes

$$-\frac{\partial \bar{E}}{\partial \bar{x}} = 3 \psi_{eff} \ln(\Lambda_i) \frac{m_{\alpha}}{m_{eff}} \frac{1}{\bar{E}} + 4 \ln(\Lambda_e) \sqrt{\frac{m_e}{\pi m_{\alpha}}} \left(\frac{m_e c^2}{T_e} \right)^{3/2} \sqrt{\bar{E}} \quad (132)$$

$$m_{eff} = \frac{1}{n_i} \sum_j n_j m_j \quad (133)$$

It is seen that the stopping power depends only weakly on the ion temperature through the ion coulomb log. The stopping power eq.(132) can be integrated

$$\int_{\bar{E}_{\alpha o}}^0 \frac{\bar{E} d\bar{E}}{A^3 + \bar{E}^{3/2}} = B \int_0^{\bar{R}_a} d\bar{x} \quad (134)$$

$$B\bar{R}_a = 2\sqrt{\bar{E}_{\alpha o}} + \frac{A}{3} \left[2\sqrt{3} \tan^{-1} \left(\frac{A - 2\sqrt{\bar{E}_{\alpha o}}}{\sqrt{3}A} \right) + \ln \left(\frac{(A - \sqrt{\bar{E}_{\alpha o}})^2 + A\sqrt{\bar{E}_{\alpha o}}}{(A + \sqrt{\bar{E}_{\alpha o}})^2} \right) - \frac{\pi}{\sqrt{3}} \right] \quad (135)$$

$$A = \left[\frac{3}{4} \psi_{eff} \frac{\ln \Lambda_i}{\ln \Lambda_e} \frac{m_\alpha}{m_{eff}} \sqrt{\frac{\pi m_\alpha}{m_e}} \right]^{1/3} \sqrt{\frac{T_e}{m_e c^2}} \quad (136)$$

$$B = 4 \ln(\Lambda_e) \sqrt{\frac{m_e}{\pi m_\alpha}} \left(\frac{m_e c^2}{T_e} \right)^{3/2} \quad (137)$$

where \bar{R}_a is the dimensionless range of an alpha particle and $\bar{E}_{\alpha o}$ is the dimensionless alpha particle initial energy found from eq.(96). The dimensionless parameters A and B are used for notational simplicity. The above range expression is only valid if the alpha particle slows down in a homogenous medium. It should be noted that a nice analytical expression cannot be found for the alpha particle range as a function of path length, $\bar{E}(\bar{x})$. Only when the energy is integrated to zero does the above expression result.

It turns out that $A \approx 4\sqrt{\frac{T_e}{m_e c^2}}$. Therefore, for small T_e (and hence small A), an expansion can be made.

$$B\bar{R}_a \approx 2\sqrt{\bar{E}_{\alpha o}} - \frac{4\pi}{3\sqrt{3}}A + \frac{A^3}{\bar{E}_{\alpha o}} \quad (138)$$

To lowest order this just becomes

$$\bar{R}_\alpha \approx 2\frac{\sqrt{\bar{E}_{\alpha o}}}{B} \quad (139)$$

$$R_a = \frac{c}{2\nu_T \ln(\Lambda_e)} \frac{\sqrt{\pi m_\alpha c^2 E_{\alpha 0}}}{(m_e c^2)^{5/2}} T_e^{3/2} \quad (140)$$

As can be seen from the definition, the quantity A can be thought of as a measure of the importance of the ions on an alpha slowing down. If the ions are ignored, then $A \Rightarrow 0$, and the range is given by eq.(140). If an equi-molar mixture of DT is assumed, this range becomes

$$R_a = 0.107 \frac{T_e^{3/2}}{\rho \ln(\Lambda)} [cm] \quad (141)$$

where $n_e = N_A \rho / 2.5$ was used (assuming pure 50/50 DT plasma). This is *precisely* the value given in Atzeni eq.(4.6), (Atzeni & Meyer-Ter-Vehn 2007). A plot of the range as determined by both eq.(135) and eq.(140) is shown in figure (2) for $n_D = n_T = 6 \cdot 10^{24} \# / cc$, $\rho = 50g/cc$, and $T_i = 100$.

As can be seen, the range calculated including thermal ion collisions is much shorter than otherwise, especially as T_e gets large. The range as calculated by numerically integrating eq.(124), using the Chandrasekhar functions, lies directly on top of the black curve when $T_i = 100$. It lies slightly above the black curve for $T_i = 10$. This shows that for these parameters, the approximate slowing down equation resulting from taking the appropriate limits of the Chandrasekhar function is very accurate. This also shows that while the range is very dependent on whether or not ions are included in the slowing down equation, it varies little with ion temperature.

An expression for the velocity as a function of time can similarly be found. Taking the appropriate limits of the Chandrasekhar function, eq.(121) becomes

$$-\frac{\partial \beta_\alpha}{\partial t} = 6\nu_T \psi_{eff} \ln(\Lambda_i) \frac{m_e^2}{m_\alpha m_{eff}} \frac{1}{\beta_\alpha^2} + \frac{4}{\sqrt{2\pi}} \nu_T \ln(\Lambda_e) \frac{m_e}{m_\alpha} \left(\frac{m_e c^2}{T_e} \right)^{3/2} \beta_\alpha \quad (142)$$

This equation can be integrated resulting in

$$\beta_\alpha(t) = [(A + \beta_{\alpha 0}^3) \exp(-3B\nu_T t) - A]^{1/3} \quad (143)$$

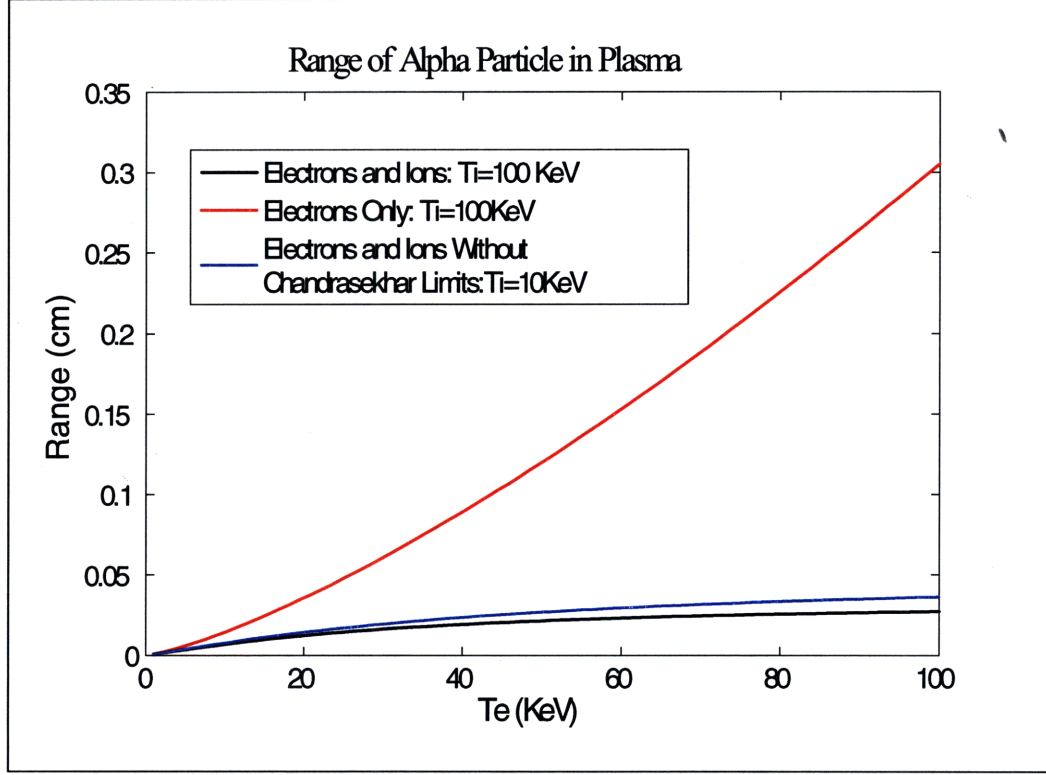


Figure 2: Range of fast alpha particles in a homogenous medium. The red curve is calculated assuming only collisions with electrons. The black curve is calculated assuming collisions with both electrons and ions, but the appropriate limits of the Chandrasekhar functions have been taken. The blue curve is calculated the same as the black, but without the simplifications of the Chandrasekhar functions and with $T_i = 10$ KeV.

$$A = 3 \sqrt{\frac{\pi}{2}} \frac{m_e}{m_{eff}} \psi_{eff} \frac{\ln(\Lambda_i)}{\ln(\Lambda_e)} \left(\frac{T_e}{m_e c^2} \right)^{3/2} \quad (144)$$

$$B = \frac{4}{\sqrt{2\pi}} \ln(\Lambda_e) \frac{m_e}{m_\alpha} \left(\frac{m_e c^2}{T_e} \right)^{3/2} \quad (145)$$

where A and B are again defined as useful dimensionless parameters. The stopping time is found by finding the time at which the alpha particle velocity becomes zero, $\beta_\alpha(t_s) = 0$.

$$t_s = \frac{1}{3B\nu_T} \ln \left[\frac{(A + \beta_{\alpha 0}^3)}{A} \right] \quad (146)$$

Taking $n_D = n_T = 2 \cdot 10^{25} \# / cc$, $\rho = 166 g / cc$, $T_i = 70$, and $T_e = 30$,

$$t_{fus} = 5.6 \cdot 10^{-11} s \quad (147)$$

$$t_s = 6.1 \cdot 10^{-12} s \quad (148)$$

where T_i was chosen near the peak of the DT reactivity. The alpha stopping time is about an order of magnitude less than the fusion time scale. Also note that evaluating T_i at the peak of the reactivity gives a minimum fusion time scale.

Finally, the fraction of energy that an alpha particle gives to electrons can be found. The rate of change of the energy of an alpha particle is

$$-\frac{\partial \bar{E}_\alpha}{\partial t} = 6\nu_T \psi_{eff} \ln(\Lambda_i) \frac{m_e}{m_{eff}} \frac{1}{\beta_\alpha} + \frac{4}{\sqrt{2\pi}} \nu_T \ln(\Lambda_e) \left(\frac{m_e c^2}{T_e} \right)^{3/2} \beta_\alpha^2 \quad (149)$$

This can be written as the sum of the rate of change of energy given to the electrons and ions

$$-\frac{\partial \bar{E}_\alpha}{\partial t} = \frac{\partial \bar{E}_i}{\partial t} + \frac{\partial \bar{E}_e}{\partial t} \quad (150)$$

Since the velocity $\beta_\alpha(t)$ is now known, the energy given to the electrons can be written

$$\bar{E}_e = \int_0^{t_s} dt \frac{4}{\sqrt{2\pi}} \nu_T \ln(\Lambda_e) \left(\frac{m_e c^2}{T_e} \right)^{3/2} \beta_\alpha^2(t) \quad (151)$$

and the fraction of energy given to the electrons, f_e ,

$$f_e = \frac{\bar{E}_e}{\bar{E}_{\alpha 0}} = \frac{4}{E_{\alpha 0} \sqrt{2\pi}} \nu_T \ln(\Lambda_e) \frac{(m_e c^2)^{5/2}}{T_e^{3/2}} \int_0^{t_s} dt [(A + \beta_{\alpha 0}^3) \exp(-3B\nu_T t) - A]^{2/3} \quad (152)$$

The integral for the electron fraction f_e results in a hypergeometric function, $F_1^2 \left[\frac{1}{3}, \frac{1}{3}, \frac{4}{3}, \varepsilon \right]$, which

is a power series in the quantity $\varepsilon \equiv \frac{A}{A+\beta_{\alpha o}^3}$.

$$f_e = \frac{4}{\sqrt{2\pi}} \ln(\Lambda_e) \frac{(m_e c^2)^{5/2}}{E_{\alpha o} T_e^{3/2}} \left[\frac{\beta_{\alpha o}^2}{2B} - \frac{A^{2/3}}{B} \left(\frac{2\pi}{3\sqrt{3}} + \varepsilon^{1/3} F_1^2 \left[\frac{1}{3}, \frac{1}{3}, \frac{4}{3}, \varepsilon \right] \right) \right] \quad (153)$$

$$F_1^2 \left[\frac{1}{3}, \frac{1}{3}, \frac{4}{3}, \varepsilon \right] = 1 + \frac{\varepsilon}{12} + O(\varepsilon^2) \quad (154)$$

In an equimolar DT plasma, the dimensionless parameters are $\psi_{eff} \approx 1.6$, $\frac{\ln(\Lambda_i)}{\ln(\Lambda_e)} \approx 1.8$, $A \approx 0.0024 \left(\frac{T_e}{m_e c^2} \right)^{3/2}$, and $\beta_{\alpha o}^3 = 8 \cdot 10^{-5}$. Therefore the quantity ε appearing in the power series is

$$\varepsilon = \frac{A}{A + \beta_{\alpha o}^3} \approx \frac{1}{1 + 0.03 \left(\frac{m_e c^2}{T_e} \right)^{3/2}} \quad (155)$$

For small electron temperature T_e , ε becomes a good expansion parameter. If $T_e \approx 10$, the parameter ε is about 0.1. Assuming that, $\varepsilon^{1/3}$, $\varepsilon \ll \frac{2\pi}{3\sqrt{3}} = 1.21$, the hypergeometric function term in the electron fraction f_e can be ignored

$$f_e = \frac{\bar{E}_e}{\bar{E}_{\alpha o}} = \frac{4}{\sqrt{2\pi}} \ln(\Lambda_e) \frac{(m_e c^2)^{5/2}}{E_{\alpha o} T_e^{3/2}} \left[\frac{\beta_{\alpha o}^2}{2B} - \frac{2\pi}{3\sqrt{3}} \frac{A^{2/3}}{B} \right] \quad (156)$$

Plugging in the dimensionless parameters A and B gives for the electron energy fraction

$$f_e = 1 - \frac{4\pi^{4/3}}{\sqrt{26}^{5/6}} \frac{\psi_{eff}^{2/3}}{(m_{eff} c^2)^{2/3} (m_e c^2)^{1/3}} \left(\frac{\ln \Lambda_i}{\ln \Lambda_e} \right)^{2/3} \frac{m_{\alpha} c^2}{E_{\alpha}} T_e \quad (157)$$

The coefficient in front of the electron temperature T_e will be defined as the 'Fraley parameter' x ,

$$x = \frac{4\pi^{4/3}}{\sqrt{26}^{5/6}} \frac{\psi_{eff}^{2/3}}{(m_{eff} c^2)^{2/3} (m_e c^2)^{1/3}} \left(\frac{\ln \Lambda_i}{\ln \Lambda_e} \right)^{2/3} \frac{m_{\alpha} c^2}{E_{\alpha}} \quad (158)$$

If the quantity xT_e is small, then the electron energy fraction can be written

$$f_e = \frac{1}{1 + xT_e} \quad (159)$$

This is the same functional form as the Fraley result, hence the definition of x as the Fraley parameter. This parameter evaluated for a homogenous DT plasma with $\ln \Lambda_e = \ln \Lambda_i$ is found to be $\approx 1/32.7$. This value is very close to the value of $1/32$ found in the empirical Fraley fit. However, this expression for the electron energy fraction f_e has been derived from first principles and a series of approximations, most significantly the approximation that the electron temperature T_e is small. However this result turns out not to be that bad for larger T_e as can be seen in figure(3). One note of significance is the dependence of the Fraley parameter x on Z_{eff} (through ψ_{eff}), and the ratio of the coulomb logarithms, which is not necessarily unity. A plot of the fraction of energy given to electrons by an alpha particle slowing down in an equimolar homogenous DT plasma is shown in figure (3). The parameters used are $n_D = n_T = 2 \cdot 10^{25} \# / cc$, $\rho = 166 g / cc$, $T_i = 70$.

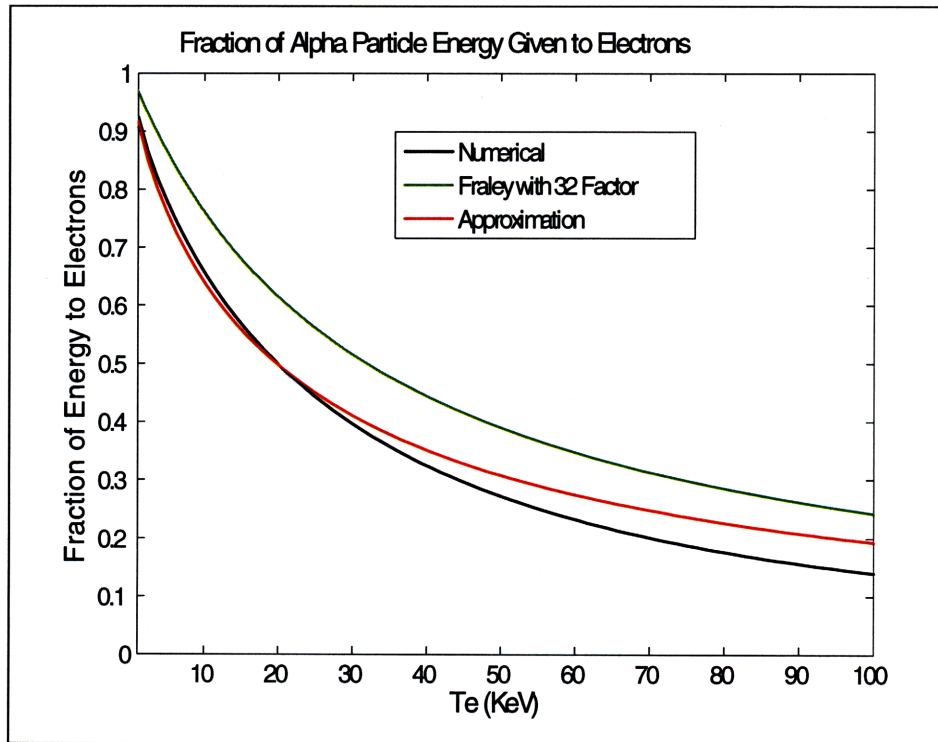


Figure 3: Fraction of fast alpha particle energy given to the plasma electrons. The green curve is the well known Fraley result. The red curve is calculated from eq.(159). The black curve is calculated numerically.

The black curve is the electron energy fraction f_e calculated by integrating eq.(149). The curve

found by integrating eq.(121) lies virtually on top of the black curve. The red curve is eq.(159) with the Fraley parameter given by eq.(158), while the green curve is eq.(159) with $x = 1/32$ (empirical Fraley fit). One can see how the approximate formula eq.(159) approaches the numerical result for small T_e : precisely the assumption under which it was derived. The main difference between the black and green curves is due the ratio of the coulomb logarithms. If the coulomb log ratio is 1, then the Fraley parameter is $1/32$. However, given the formulas from Atzeni for the coulomb logs, eq.(5) and eq.(6), the Fraley parameter is $1/21$. It clear that this ratio has a noticeable effect on the energy splitting fractions f_e and f_i . More importantly, assuming that the ion coulomb log equals the electron coulomb log underestimates the energy given to ions throughout the entire burn, as the ion coulomb log is almost always larger than the electron coulomb log.

4.3 Geometry

In this section, the fraction of alpha energy given to the ions, $f_{\alpha i}$, and the fraction of alpha energy given to the electrons, $f_{\alpha e}$, will be derived for the specific case of the isothermal rarefaction model where not all of the alpha particles actually stop in the fuel sphere. The zero-D model of an ICF capsule consists of a homogenous sphere of plasma at specific ion and electron temperatures and densities. The radius of the homogenous sphere is R , which is just the radius of the inward moving rarefaction wave. At any given point in the sphere, alpha particles are emitted isotropically from fusion reactions. Once an alpha is emitted, it follows a straight path in a certain direction until it travels a distance R_α , which is the range of an alpha particle in the homogenous plasma, or until it leaves the sphere. The alpha particle loses energy to the plasma along its path. The energy of an alpha particle is given by a function of the path length the alpha has traveled, $E_\alpha(x)$. This is precisely the function found by integrating eq.(124) from $x' = 0$ to $x' = x$. This function is $E_\alpha \approx 3.5$ Mev at $x = 0$ and zero at $x = R_\alpha$. Given $E_\alpha(x)$, the fraction of total alpha power which is delivered inside the sphere can be found. It is actually easier to first calculate the total instantaneous power that leaves the sphere in the form of alpha particle kinetic energy. This is given by

$$P_{lost} = \int d\Omega dV E_\alpha(x[\mathbf{r}, \boldsymbol{\Omega}]) N_\alpha \quad (160)$$

This expression involves a volume integral over the sphere. N_α is the rate of production of alpha particles which are emitted in direction $\mathbf{\Omega}$ at point \mathbf{r} . Due to the homogenous assumption of the model, N_α does not depend on $\mathbf{\Omega}$ or \mathbf{r} . Clearly, $\int d\Omega dV N_\alpha = 16\pi^2 R^3 N_\alpha / 3$ is the total rate of production of alpha particles in the sphere and $N_\alpha = \frac{n_D n_T \langle \sigma v \rangle}{4\pi}$. Each alpha particle produced at point \mathbf{r} in direction $\mathbf{\Omega}$ travels a distance $x[\mathbf{r}, \mathbf{\Omega}]$ upon reaching the surface of the sphere, provided $R_a > x[\mathbf{r}, \mathbf{\Omega}]$. The energy that these particles have when they reach the surface is $E_\alpha(x[\mathbf{r}, \mathbf{\Omega}])$, and this energy is deposited in the rarefacted material which is not considered in this model. Of course, $E_\alpha(x[\mathbf{r}, \mathbf{\Omega}])$ is zero if $R_a \leq x[\mathbf{r}, \mathbf{\Omega}]$. Due to spherical symmetry, a spherical coordinate system can be chosen at a particular point \mathbf{r} with the z-axis pointing radially outward. This point can be moved around on the surface of constant radius r with the z axis always pointing radially outward without changing the geometry. Therefore, the angular part of the volume integral just gives a 4π factor. In other words, the calculation can be done for one point on this spherical surface because it is the same for all other points on this same surface. Krokhin and Rozanov perform a very similar calculation for constant alpha stopping power(O. N. Krokhin & V. B. Rozanov, *Soviet Journal of Quantum Electronics*, vol. 2, 393–394 (1973) 1973).

At radius r with $\hat{\mathbf{z}} = \hat{\mathbf{r}}$ and with $\mathbf{\Omega}$ being defined by the angles θ and ϕ , the power is

$$P_{lost} = 4\pi \int r^2 dr d\phi \sin(\theta) d\theta E_\alpha(x[r, \theta, \phi]) N_\alpha \quad (161)$$

Finally, this is also independent of the angle ϕ , resulting in

$$P_{lost} = 8\pi^2 \int r^2 dr \sin(\theta) d\theta E_\alpha(x[r, \theta]) N_\alpha \quad (162)$$

$$x[r, \theta] = \sqrt{R^2 + r^2 (\cos(\theta)^2 - 1)} - r \cos(\theta) \quad (163)$$

The geometry for this calculation is shown in figure (4), and was worked out by O. N. Krokhin and V. B. Rozanov(Krokhin & Rozanov 1973).

Changing variables to dimensionless radius $\rho = \frac{r}{R}$, $\mu = \cos(\theta)$, and dimensionless path length

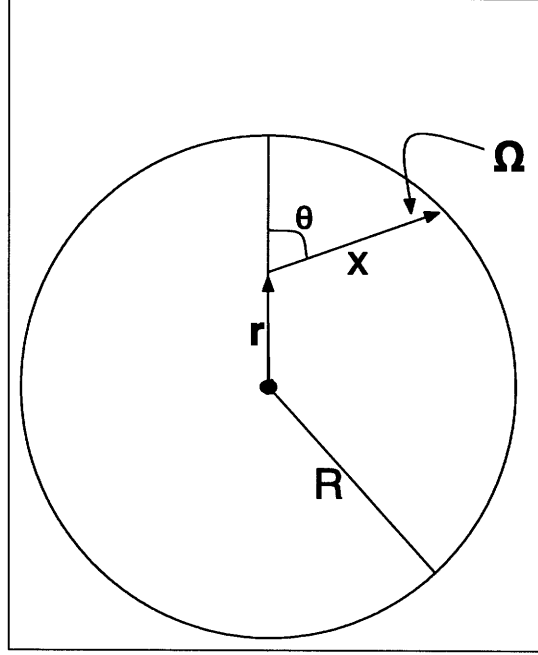


Figure 4: The geometry for the calculation of the fraction of fast alpha energy that leaves the fuel sphere.

$$y = \frac{x}{R},$$

$$P_{lost} = 8\pi^2 N_\alpha R^3 \int_0^1 \rho^2 d\rho \int_{-1}^1 d\mu E_\alpha [y(\rho, \mu)] \quad (164)$$

$$y = \sqrt{1 + \rho^2 (\mu^2 - 1)} - \rho\mu \quad (165)$$

Since the alpha particle energy as a function of path length, $E[y]$, is explicitly known, it is convenient to change integration variables from θ to y .

$$dy = \rho \left(\frac{\rho\mu}{\sqrt{1 + \rho^2 (\mu^2 - 1)}} - 1 \right) d\mu \quad (166)$$

$$P_{lost} = -8\pi^2 N_\alpha R^3 \int_{y_{min}}^{y_{max}} dy \int_1^{1-y} \rho d\rho \left(\frac{\rho\mu[y, \rho]}{\sqrt{1 + \rho^2 (\mu[y, \rho]^2 - 1)}} - 1 \right)^{-1} E_\alpha(y) \quad (167)$$

$$P_{lost} = 4\pi^2 N_\alpha R^3 \int_{y_{\min}}^{y_{\max}} dy \int_{1-y}^1 \rho d\rho (y^2 + 1 - \rho^2) \frac{E_\alpha(y)}{y^2} \quad (168)$$

The limits on ρ should be noted here. y is defined as the distance from the point in question to the surface of the sphere. Clearly, given y , the smallest ρ can be is $1 - y$. This occurs at $\mu = 1$. The maximum ρ can be is 1. Therefore, the limits on ρ are $1 - y$ to 1. The lower limit on y is zero. The upper limit on x is the minimum of the range R_α and twice the radius R , $\min(2R, R_\alpha)$. The upper limit on x is really $2R$, the diameter of the sphere, as this is the largest that x could be. However, since $E_\alpha(x) = 0$ for $x > R_\alpha$, there is an effective limit of R_a . In terms of y this gives

$$P_{lost} = 4\pi^2 N_\alpha R^3 \int_0^{\min(2, R_a/R)} dy \int_{1-y}^1 \rho d\rho (y^2 + 1 - \rho^2) \frac{E_\alpha(y)}{y^2} \quad (169)$$

Finally, the integral over the dimensionless radius ρ can be done

$$P_{lost} = 4\pi^2 N_\alpha R^3 \int_0^{\min(2, R_a/R)} dy \left(1 - \frac{y^2}{4}\right) E_\alpha(y) \quad (170)$$

This gives for the fraction of power deposited in the sphere, $1 - \frac{P_{lost}}{P_\alpha}$ where $P_\alpha = 16\pi^2 R^3 N_\alpha E_{\alpha 0}/3$,

$$f_{in} = 1 - \frac{3}{4} \int_0^{\min(2, R_a/R)} dy \left(1 - \frac{y^2}{4}\right) \frac{E_\alpha(y)}{E_{\alpha 0}} \quad (171)$$

O. N. Krokhin and V. B. Rozanov (Krokhin & Rozanov 1973) arrive at this same result. The fraction of alpha particles that stay in the sphere for $R_a > 2R$ is

$$f_{n\alpha} = 1 - \frac{3}{4} \int_0^2 dy \left(1 - \frac{y^2}{4}\right) = 0 \quad (172)$$

as expected. For $R_a < 2R$, the fraction that stay in the sphere is

$$f_{n\alpha} = 1 - \frac{3}{4} \int_0^{R_a/R} dy \left(1 - \frac{y^2}{4}\right) = 1 - \frac{3}{4} \int_0^{R_a/R} dy \left(1 - \frac{y^2}{4}\right) = 1 - \frac{3R_a}{4R} + \frac{1}{16} \left(\frac{R_a}{R}\right)^3 \quad (173)$$

The fraction of energy given to the ions can be found as follows. The energy of an alpha particle as a function of distance along its path is found by integrating eq.(128) or eq.(132). Take

for example the approximate eq.(132). This can be written as

$$-\frac{\partial \bar{E}_\alpha}{\partial \bar{x}} = \frac{\partial \bar{E}_i}{\partial \bar{x}} + \frac{\partial \bar{E}_e}{\partial \bar{x}} \quad (174)$$

$$\frac{\partial \bar{E}_i}{\partial \bar{x}} = 3 \psi_{eff} \ln(\Lambda_i) \frac{m_\alpha}{m_{eff}} \frac{1}{\bar{E}_\alpha(\bar{x})} \quad (175)$$

This can be integrated giving

$$\bar{E}_i(\bar{x}) = \int_0^{\bar{x}'} 3 \psi_{eff} \ln(\Lambda_i) \frac{m_\alpha}{m_{eff}} \frac{d\bar{x}'}{\bar{E}_\alpha(\bar{x}')} \quad (176)$$

and similarly for the electrons. Now that $E_i(x)$ is known, the fraction of fast alpha energy given to the ions is

$$f_{\alpha i} = \frac{P_{ions}}{P_{produced}} = \left[\begin{array}{l} 4\pi^2 N_\alpha R^3 \int_0^{\min(2R, R_a/R)} dy \left(1 - \frac{y^2}{4}\right) E_i(y) \\ + f_{n\alpha} E_i(R_\alpha/R) \frac{16\pi^2 R^3 N_\alpha}{3} \end{array} \right] \frac{3}{16\pi^2 R^3 N_\alpha E_{\alpha o}} \quad (177)$$

$$f_{\alpha i} = \frac{3}{4R} \int_0^{\min(2R, R_a)} dx \left(1 - \frac{1}{4} \left(\frac{x}{R}\right)^2\right) \frac{E_i(x)}{E_{\alpha o}} + f_{n\alpha} \frac{E_i(R_\alpha)}{E_{\alpha o}} \quad (178)$$

Finally, the fraction of alpha power delivered to the fuel sphere f_{in} , the fraction of alpha particles that stay in the sphere $f_{n\alpha}$, the fraction of energy given to the ions $f_{\alpha i}$, and the fraction of energy given to the electrons $f_{\alpha e}$ is

$$f_{in} = 1 - \frac{3}{4R} \int_0^{\min(2R, R_a)} dx \left(1 - \frac{1}{4} \left(\frac{x}{R}\right)^2\right) \frac{E_\alpha(x)}{E_{\alpha o}} \quad (179)$$

$$f_{n\alpha} = 1 - \frac{3 R_a}{4 R} + \frac{1}{16} \left(\frac{R_a}{R}\right)^3 \quad R_a < 2R \quad (180)$$

$$f_{n\alpha} = 0 \quad R_a > 2R \quad (181)$$

$$f_{\alpha i} = \frac{3}{4R} \int_0^{\min(2R, R_a)} dx \left(1 - \frac{1}{4} \left(\frac{x}{R}\right)^2\right) \frac{E_i(x)}{E_{\alpha o}} + f_{n\alpha} \frac{E_i(R_\alpha)}{E_{\alpha o}} \quad (182)$$

$$f_{\alpha e} = \frac{3}{4R} \int_0^{\min(2R, R_\alpha)} dx \left(1 - \frac{1}{4} \left(\frac{x}{R} \right)^2 \right) \frac{E_e(x)}{E_{\alpha o}} + f_{n\alpha} \frac{E_e(R_\alpha)}{E_{\alpha o}} \quad (183)$$

These are the energy splitting fractions used in the isothermal rarefaction model. Note that in the limit of a very large sphere, $R \Rightarrow \infty$, the fraction of alpha particles that stay within the burning fuel approaches 1 and the energy splitting fractions become

$$f_{\alpha i} = \frac{E_i(R_\alpha)}{E_{\alpha o}} \quad (184)$$

$$f_{\alpha e} = \frac{E_e(R_\alpha)}{E_{\alpha o}} \quad (185)$$

which is what they would be in an infinite homogenous medium.

5 Radiation

There are two main limits where the radiation can be treated in a simple fashion. When the photon mean free path, including reabsorption and scattering, is very short compared to system scale lengths, the system is optically thick. In this situation, the radiation diffusion approximation is valid and the radiation pressure is isotropic and equal to a third the radiation energy density. Furthermore, the radiation tends to be driven to an equilibrium distribution, and equations governing the macroscopic quantities given by the moments of the photon distribution determine the photon behavior. Conventionally the photon equilibrium distribution is assumed to be black body. This assumption leads to significant errors in burn dynamics. A new photon treatment, called 4T theory (Kim Molvig, Marv Alme, Robert Webster & Conner Galloway, *Physics of Plasmas*, vol. 16, 023301 (2009) 2009), has been developed to accurately describe the radiation during runaway burn in optically thick media, and is discussed below.

When the photon mean free path is very long compared to system scale lengths, emission dominates scattering and absorption. Photons tend to free stream out of the system at the speed of light, and the energy loss from the electrons is just volumetric Bremsstrahlung loss at temperature

T_e . At system length scales that are comparable with an average absorption mean free path (Planck mean free path), absorption can be treated without too much difficulty provided the Thomson mean free path is still large. Typical ICF capsules operate in the optically thin regime with small but noticeable reabsorption, and this regime is what will be treated in the isothermal model. A discussion of the optically thick case is first given for completeness.

It is conventionally understood that the photon distribution in a quasi-steady optically thick medium is black body. This can be seen from a kinetic point of view, where the full Bremsstrahlung operator in the photon kinetic equation drives the photons to a black body distribution. This black body distribution is completely characterized by a single temperature, which under matter-radiation equilibrium is the electron temperature. Gradients of the photon black body distribution give rise to photon energy fluxes in the diffusion limit. Because the photon distribution depends only on temperature, the photon energy fluxes are proportional to the temperature gradients, and the proportionality constant involves the Rosseland mean opacity. A strong assumption is commonly made that the photon distribution can depart from equilibrium with the electrons and be described by a black body distribution with a separate radiation temperature. However, this conventional assumption leads to significant errors in burn dynamics. During burn Compton scattering can dominate Bremsstrahlung, and the equilibrium photon distribution can shift from black body to a *diluted Planckian* (Bose-Einstein distribution with non-zero chemical potential). Since scattering cannot produce photons, the heating of the photons that accompanies Compton scattering when the electron temperature is greater than the radiation temperature, $T_e > T_R$, moves the photons to higher energy, leaving a *diluted* region at low energies. When Compton scattering is the only matter-radiation interaction process in an infinite, homogeneous plasma, it drives the photon distribution to a diluted Planckian. In such a situation the Compton energy exchange between matter and radiation is effectively eliminated. This is in contrast to the energy exchange rate computed with the 3T equations (assumption of black body radiation at radiation temperature T_R) which has a very large Compton exchange rate. Even with the other matter-radiation interaction processes included, the reduction of the Compton cooling of the electrons can be substantial (Molvig *et al.* 2009). This is the situation addressed by 4T theory. The isothermal rarefaction model does not cover optically

thick media.

The dominant interaction of radiation and matter in typical ICF systems is Bremsstrahlung. Since starting temperatures for burn from a compressed state are of the order of a few KeV, the hydrogen plasma is fully ionized. Therefore there are only free-free transitions involved in photon absorption and production. Consider a homogenous system at some temperature T where at time $t = 0$ there is no radiation field. Immediately, there will be spontaneous emission occurring uniformly in the medium. The rate of production of photons per unit time, angle, volume, and photon energy is given by the emission coefficient j_ϵ (the conventional emission coefficient has units of energy, not number. Here a particle distribution function approach is taken). However once the radiation field builds up, the processes of absorption and stimulated emission, which are proportional to the photon distribution f , occur. The rate of absorption less stimulated emission for a given photon frequency is given by $c\kappa_\epsilon$, and a mean free path for this process for a given photon frequency is $1/\kappa_\epsilon$, where κ_ϵ is the absorption coefficient corrected for stimulated emission. It can be shown that if the system mean free path is much longer than $1/\kappa_\epsilon$ for the relevant frequency range, then the radiation field builds up toward black body on a time scale of order $1/c\langle\kappa_\epsilon\rangle$ (Ya. B. Zel'dovich & Yu. P. Raizer, *Physics of Shock Waves and High-Temperature Hydrodynamic Phenomena* (Mineola, New York: Dover Publications, Inc., 2002) 2002). Here the averaging is with respect to a black body photon distribution at temperature T . This is related to the Planck mean absorption coefficient $1/c\langle\kappa_\epsilon\rangle = 1/\kappa_p c$.

For a system whose length scales are comparable to an average photon mean free path, the photon distribution never has a chance to fully build up to black body. Photons that would be reabsorbed are lost through the system boundaries. These photons that are lost take energy with them, and this constitutes a radiation energy loss from the system. If L is a scale length of the system, and if L/c and $1/\langle\kappa_\epsilon\rangle$ time scales are short compared to all other time scales, then the photon distribution can be assumed to be in quasi equilibrium at all times. This is typically the case for ICF.

Within the homogenous fuel sphere, photons are isotropically produced and then free stream in a straight line until they leave the sphere or are reabsorbed. It is assumed that once photons

leave the sphere, they are not re-radiated back due to the longer mean free paths in the rarefacted material. This of course is an approximation, but it is conservative. An exact solution of the transport equation for the photon distribution as a function of position, energy, and angle inside the ICF sphere can be found from the full Bremsstrahlung operator, including absorption and stimulated emission, assuming the fuel sphere is homogenous and the photon distribution is always in quasi-steady state. Once the photon distribution is found, the flux of energy leaving the sphere can be calculated and the radiative power loss term P_{rad} determined.

The Bremsstrahlung operator is (A.S. Kompaneets, *Soviet Phys. JETP*, vol. 4, 730 (1957) 1957)

$$C_B = \frac{1}{4\pi} \frac{\nu_B n_e}{T_e} \sqrt{\frac{m_e c^2}{2T_e}} \frac{1}{\varepsilon} e^{-\varepsilon/2} K_0(\varepsilon/2) [1 - n_\gamma (e^\varepsilon - 1)]$$

where n is the photon occupation number. The photon kinetic equation is

$$\frac{\partial f}{\partial t} + c \hat{\mathbf{n}} \cdot \nabla f = C_B = j_\varepsilon - c \kappa_\varepsilon f$$

where f is the number of photons at position r at time t with energy ε moving in direction $\hat{\mathbf{n}}$ in phase space volume $\Delta \mathbf{r} \Delta \varepsilon d\Omega$, and

$$j_\varepsilon = \frac{1}{4\pi} \frac{\nu_B n_e}{T_e} \sqrt{\frac{m_e c^2}{2T_e}} \frac{1}{\varepsilon} e^{-\varepsilon/2} K_0(\varepsilon/2)$$

$$\kappa_\varepsilon = \frac{\nu_B}{c} \frac{n_e}{N_\gamma(T_e)} \sqrt{\frac{m_e c^2}{2T_e}} \frac{1}{\varepsilon^3} e^{-\varepsilon/2} K_0(\varepsilon/2) (e^\varepsilon - 1)$$

$$N_\gamma(T_e) = \frac{8\pi T_e^3}{h^3 c^3} \quad (186)$$

$$\nu_B = \frac{4}{\pi^{3/2}} Z_{eff} \alpha \nu_T \quad (187)$$

where j_ε and κ_ε are the absorption and emission coefficients that are assumed constant across the ICF sphere, N_γ is a density and comes from the photon density of states, K_0 is the modified bessel function of the second kind, and ε is a dimensionless photon energy $\frac{h\nu}{T_e}$. The fine structure constant is

$\alpha = 1/137$. The units of κ_ε are carried by c and a bremsstrahlung rate ν_B , through the Thompson rate $\nu_T = n_e c \sigma_T$. The absorption coefficient can also be written as

$$\kappa_\varepsilon = \frac{\nu_B}{c} n_e r_e^3 \frac{\pi^2}{\sqrt{2}\alpha^3} \left(\frac{m_e c^2}{T_e} \right)^{7/2} \frac{1}{\varepsilon^3} e^{-\varepsilon/2} K_0(\varepsilon/2) (e^\varepsilon - 1) \quad (188)$$

where α is the fine structure constant and r_e is the classical electron radius. Note that this definition of κ_ε includes stimulated emission. The quasi-equilibrium assumption leads to

$$\hat{\mathbf{n}} \cdot \nabla f(\varepsilon, \hat{\mathbf{n}}, \mathbf{r}) = \frac{1}{c} j_\varepsilon(\varepsilon) - \kappa_\varepsilon(\varepsilon) f(\varepsilon, \hat{\mathbf{n}}, \mathbf{r}) \quad (189)$$

where the functional dependences are made explicit. The term on the left hand side is a directional derivative. This can be formally solved by using an integrating factor. In general $j_\varepsilon(\varepsilon, \hat{\mathbf{n}}, \mathbf{r}')$ can depend on position and angle. If \mathbf{r}' is the vector that locates the original source of a photon (determined by j_ε) which free streams in direction $\hat{\mathbf{n}}$ a distance y to a location \mathbf{r} , and further has probability per unit length of being absorbed during its travel to point \mathbf{r} given by $\kappa_\varepsilon(\varepsilon)/c$, then eq.(189) can be integrated as

$$\begin{aligned} \frac{\partial}{\partial y} (f \exp[\kappa_\varepsilon(\varepsilon) \mathbf{r} \cdot \hat{\mathbf{n}}]) &= \frac{1}{c} j_\varepsilon(\varepsilon) \exp[\kappa_\varepsilon(\varepsilon) \mathbf{r} \cdot \hat{\mathbf{n}}] \\ f &= \int_0^\infty dy \frac{1}{c} j_\varepsilon(\varepsilon, \hat{\mathbf{n}}, \mathbf{r} - y\hat{\mathbf{n}}) \exp[-\kappa_\varepsilon(\varepsilon) y] \end{aligned} \quad (190)$$

This expression can be simplified by taking into account spherical symmetry. At a given field point \mathbf{r} , a certain number of photons are propagating in direction $\hat{\mathbf{n}}$. In the absence of scattering, the photons traveling in this direction were emitted back along the $-\hat{\mathbf{n}}$ direction. The variable y measures this distance back along this ray. The integral in eq.(190) sums up the sources from all the points along this ray that contribute to the number of photons propagating in direction $\hat{\mathbf{n}}$ at point \mathbf{r} . The exponential takes into account that the further a photon has to travel, the more likely it is to be absorbed. For this ICF model j_ε is constant in the sphere and zero outside. Therefore eq.(190) can be solved as follows. Because of isotropy and homogeneity of j_ε and κ_ε , choose the vector \mathbf{r} to point along the z-axis in spherical coordinates. Because of spherical symmetry, the photon

distribution will be independent of ϕ and only depend on θ , thus the problem can be reduced to geometry on a circle. At the point r , let θ define the direction $\hat{\mathbf{n}}$, measuring the angle from $\hat{\mathbf{r}}$. Let y be the distance from the point at r in the $-\hat{\mathbf{n}}$ direction to the surface of the sphere. This distance is given by the law of cosines and the quadratic formula

$$y = r \cos(\theta) + \sqrt{R^2 - r^2 + r^2 \cos^2(\theta)}$$

When $\theta = 0$ this distance is $y = R + r$, when $\theta = \frac{\pi}{2}$ it is $y = \sqrt{R^2 - r^2}$, and when $\theta = \pi$ it is $y = R - r$. Over this distance y , j_ε is constant and eq.(190) becomes

$$f(\varepsilon, \theta, r) = \frac{1}{c} j_\varepsilon(\varepsilon) \int_0^y dy' \exp[-\kappa_\varepsilon(\varepsilon) y'] = \frac{j_\varepsilon(\varepsilon)}{c\kappa_\varepsilon(\varepsilon)} (1 - \exp[-\kappa_\varepsilon(\varepsilon) y])$$

$$f(\varepsilon, \theta, r) = \frac{j_\varepsilon(\varepsilon)}{c\kappa_\varepsilon(\varepsilon)} \left(1 - \exp \left[-\tau(\varepsilon) \left(\frac{r}{R} \cos(\theta) + \sqrt{1 - \frac{r^2}{R^2} \sin^2(\theta)} \right) \right] \right) \quad (191)$$

$$\tau(\varepsilon) = R\kappa_\varepsilon(\varepsilon) \quad (192)$$

The distribution function evaluated at $r = R$ is

$$f(\varepsilon, \theta) = \frac{j_\varepsilon(\varepsilon)}{c\kappa_\varepsilon(\varepsilon)} (1 - \exp[-\tau(\varepsilon) (\cos(\theta) + |\cos(\theta)|)]) \quad (193)$$

As expected, if θ is greater than $\pi/2$ (corresponding to a photon coming from outside into the sphere), $f(\varepsilon, \theta)$ is zero. The total energy produced in the sphere equals the total energy which leaves the sphere through its surface. The total sphere power loss is

$$V \frac{\partial E_\gamma}{\partial t} = T_e^2 \int \int \int \varepsilon d\varepsilon d\Omega dV_{sphere} (j_\varepsilon - c\kappa_\varepsilon f) \quad (194)$$

Using eq.(189) this becomes

$$V \frac{\partial E_\gamma}{\partial t} = T_e^2 \int \int \int \varepsilon d\varepsilon d\Omega dV_{sphere} c \hat{\mathbf{n}} \cdot \nabla f = c T_e^2 \int \int \int \varepsilon d\varepsilon d\Omega \oint d\mathbf{A} \cdot \hat{\mathbf{n}} f \quad (195)$$

$$= 4\pi R^2 c T_e^2 \int \int \varepsilon d\varepsilon d\Omega \cos(\theta) f \quad (196)$$

The power loss is

$$P_\gamma = 8\pi^2 c R^2 T_e^2 \int_0^\infty \varepsilon d\varepsilon \int_0^{\pi/2} d\theta \sin(\theta) \cos(\theta) f(\varepsilon, \theta) \quad (197)$$

Evaluating the angular integral

$$\int_0^{\pi/2} d\theta \sin(\theta) \cos(\theta) f(\varepsilon, \theta) \quad (198)$$

$$= \frac{j_\varepsilon(\varepsilon)}{c \kappa_\varepsilon(\varepsilon)} \left(\int_0^{\pi/2} d\theta \sin(\theta) \cos(\theta) - \int_0^{\pi/2} d\theta \sin(\theta) \cos(\theta) \exp[-2\tau(\varepsilon) \cos(\theta)] \right) \quad (199)$$

$$= \frac{j_\varepsilon(\varepsilon)}{\kappa_\varepsilon(\varepsilon)} \left(\int_0^1 dx x - \int_0^1 dx x \exp[-2\tau(\varepsilon) x] \right) \quad (200)$$

$$= \frac{j_\varepsilon(\varepsilon)}{c \kappa_\varepsilon(\varepsilon)} \left(\frac{1}{2} - \frac{1 - (1 + 2\tau(\varepsilon)) \exp[-2\tau(\varepsilon)]}{4\tau(\varepsilon)^2} \right) \quad (201)$$

results in

$$P_\gamma = 4\pi R^2 \sigma_{SB} T_e^4 \left(1 - \frac{15}{\pi^4} \int_0^\infty d\varepsilon \frac{\varepsilon^3}{(e^\varepsilon - 1)} \frac{1 - (1 + 2\tau(\varepsilon)) \exp[-2\tau(\varepsilon)]}{2\tau(\varepsilon)^2} \right) \quad (202)$$

The two limits of $\tau(\varepsilon) \Rightarrow \infty$ and $\tau(\varepsilon) \Rightarrow 0$, corresponding to an optically thick and thin system respectively, can be checked. The first limit is easy to see. In this limit the integral term vanishes and

$$F_\varepsilon = 4\pi R^2 \sigma_{SB} T_e^4 \quad (203)$$

which is just the power emitted by a black body multiplied by the surface area. This is expected when the optical depth is very small compared to the radius of the capsule. In the other limit

$$P_\gamma = 4\pi R^2 \sigma_{SB} T_e^4 \left(1 - \frac{15}{\pi^4} \int_0^\infty d\varepsilon \frac{\varepsilon^3}{(e^\varepsilon - 1)} \left(1 - \frac{4}{3} \tau(\varepsilon) + O(\tau^2) \right) \right) \quad (204)$$

$$P_\gamma = 4\pi R^2 \sigma_{SB} T_e^4 \frac{15}{\pi^4} \int_0^\infty d\varepsilon \frac{\varepsilon^3}{(e^\varepsilon - 1)} \frac{4}{3} \tau(\varepsilon) \quad (205)$$

$$P_\gamma = \frac{4}{3}\pi R^3 \frac{\nu_B n_e}{T_e} \sqrt{\frac{m_e c^2}{2T_e}} T_e^2 \int_0^\infty d\varepsilon e^{-\varepsilon/2} K_0(\varepsilon/2) \quad (206)$$

$$P_\gamma = \frac{4}{3}\pi R^3 \frac{\nu_B n_e}{T_e} \sqrt{\frac{m_e c^2}{2T_e}} T_e^2 \cdot 2 \quad (207)$$

This is precisely the total energy moment assuming pure emission,

$$\Rightarrow T_e^2 \int \int \int \varepsilon d\varepsilon d\Omega dV_{sphere} j_\varepsilon \quad (208)$$

which is expected in the limit of an optically thin capsule. The final radiation energy loss term is given by

$$P_{rad} = \frac{3}{R} \sigma_{SB} T_e^4 \left(1 - \frac{15}{\pi^4} \int_0^\infty d\varepsilon \frac{\varepsilon^3}{(e^\varepsilon - 1)} \frac{1 - (1 + 2\tau(\varepsilon)) \exp[-2\tau(\varepsilon)]}{2\tau(\varepsilon)^2} \right) \quad (209)$$

$$\tau(\varepsilon) = \frac{R}{c} \nu_B \frac{n_e}{N_\gamma(T_e)} \sqrt{\frac{m_e c^2}{2T_e}} \frac{1}{\varepsilon^3} e^{-\varepsilon/2} K_0(\varepsilon/2) (e^\varepsilon - 1) \quad (210)$$

It should be noted again that this expression is valid only in the thin to marginally thick limit. For optically thick systems, scattering can be important and the quasi static assumption no longer holds. This expression for the radiation power loss P_{rad} is used in the isothermal rarefaction model code.

6 Simulation Results of the Isothermal Rarefaction Model

The equations of the isothermal rarefaction model can now be written down in full including fusion heating by alpha particles and cooling of the electrons through Bremsstrahlung. The independent variables are the electron and ion internal energy densities E_e and E_i ; the number densities of deuterons, tritons, and thermal alpha particles within the burning fuel sphere n_D , n_T , and n_α ; and the total particle numbers of deuterons, tritons and thermal alphas, N_D , N_T , and N_α . The

equations for the energy densities are

$$\frac{\partial E_i}{\partial t} = \left[\left(\left(Q + \frac{\langle \sigma v \varepsilon \rangle}{\langle \sigma v \rangle} \right) m_n + \frac{3}{2} T_i m_\alpha \right) \frac{f_{\alpha i} \langle \sigma v \rangle}{m_n + m_\alpha} - \left(\frac{3}{2} T_i \langle \sigma v \rangle + \langle \sigma v \varepsilon \rangle \right) \right] n_D n_T - P_{ie} - P_{cond}^i \quad (211)$$

$$\frac{\partial E_e}{\partial t} = \left(\left(Q + \frac{\langle \sigma v \varepsilon \rangle}{\langle \sigma v \rangle} \right) m_n + \frac{3}{2} T_i m_\alpha \right) \frac{f_{\alpha e} n_D n_T \langle \sigma v \rangle}{m_n + m_\alpha} + P_{ie} - P_{rad} - P_{cond}^e \quad (212)$$

where Q is the reaction energy. The fraction of fast alpha energy given to the ions and electrons, $f_{\alpha i}$ and $f_{\alpha e}$, are given by eqs.(182) and (183), and the electron-ion energy exchange P_{ie} , the electron and ion conduction losses P_{cond}^e and P_{cond}^i , and the radiation power loss P_{rad} are given by eqs.(4), (9), (10) and (209). The equations for the number densities are

$$\frac{\partial n_D}{\partial t} = -n_D n_T \langle \sigma v \rangle \quad (213)$$

$$\frac{\partial n_T}{\partial t} = -n_D n_T \langle \sigma v \rangle \quad (214)$$

$$\frac{\partial n_\alpha}{\partial t} = f_{n\alpha} n_D n_T \langle \sigma v \rangle \quad (215)$$

where the fraction of fast alpha particles that stay within the burning sphere, $f_{n\alpha}$, is given by eq.(180). The equations for the total particle numbers are

$$\frac{\partial N_D}{\partial t} = -V n_D n_T \langle \sigma v \rangle \quad (216)$$

$$\frac{\partial N_T}{\partial t} = -V n_D n_T \langle \sigma v \rangle \quad (217)$$

$$\frac{\partial N_\alpha}{\partial t} = V n_D n_T \langle \sigma v \rangle \quad (218)$$

$$V = \frac{4\pi}{3} R^3 \quad (219)$$

$$\frac{\partial R}{\partial t} = -v_r \quad (220)$$

where v_r is the velocity of the rarefaction wave front eq.(22). Some of the dependent variables written here for clarity are the total ion and electron number densities n_i and n_e , the mass density

ρ , the ion pressure P_i , and the effective ion mass m_{eff} .

$$n_i = n_D + n_T + n_\alpha \quad (221)$$

$$n_e = n_D + n_T + 2n_\alpha \quad (222)$$

$$\rho = m_D n_D + m_T n_T + m_\alpha n_\alpha \quad (223)$$

$$P_i = n_i T_i \quad (224)$$

$$m_{eff} = \frac{\rho}{n_i} \quad (225)$$

The equations above were solved in Matlab. The initial conditions that one sets in the code are T_i , T_e , n_D , n_T , and R . Equivalently, one may specify initial fuel ρR , the total mass (assuming equal molar DT mixture), and the temperatures. For all of the simulations, an initial equi-molar mixture of DT was assumed $n_D = n_T$. The code stops running when either the ion temperature falls below 2 KeV, or the radius of the rarefaction wave reaches zero. Two specific cases were run. The first case is a configuration with a robust ρR and strong runaway burn, while the second case is more marginal. After these are discussed, a plot of burn fractions as a function of ρR for many different initial conditions is presented.

Shown below are a series of plots as a function of time for the initial conditions $T_i = T_e = 5$ KeV, $R = 0.01$ cm, $n_D = n_T = 5 \times 10^{25}$ #/cc, $\rho = 418$ g/cc, total mass $m = 1.7$ mg, and $\rho R = 4.2$ g/cm². Burnup is defined as the fraction $Y = \frac{N_\alpha}{N_{p0}}$ evaluated at the end of the run. Here N_α is the total number of alpha particles that were produced during the burn, and N_{p0} is the total number of initial DT pairs. This is just equal to N_{D0} and N_{T0} because $n_{D0} = n_{T0}$.

The ion and electron temperatures are shown for this run in figure (5), and the radius of the rarefaction wave is shown in figure (6). It takes about a hundredth of a nanosecond for runaway burn to begin. During this time, the rarefaction wave proceeds inwards relatively slowly as the fuel is slowly heated. As can be seen in figure (9), most of the alpha particles stop in the fuel sphere and predominantly heat the electrons. The fuel radius R has only shrunk by a small

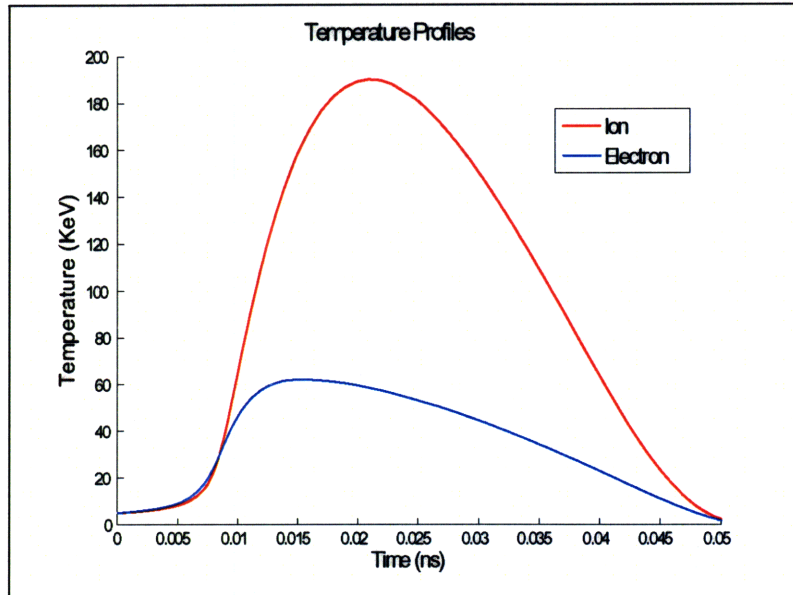


Figure 5: Ion and Electron Temperature Profiles

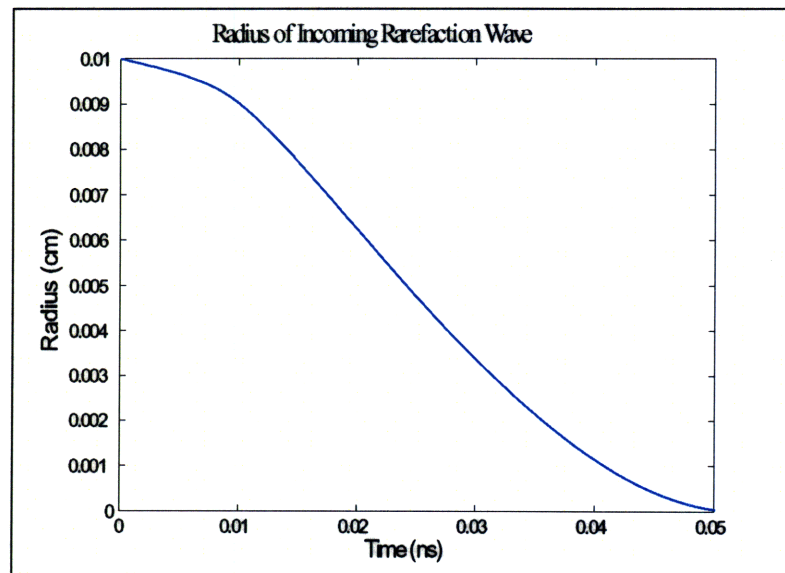


Figure 6: Radius of Incoming Rarefaction Wave

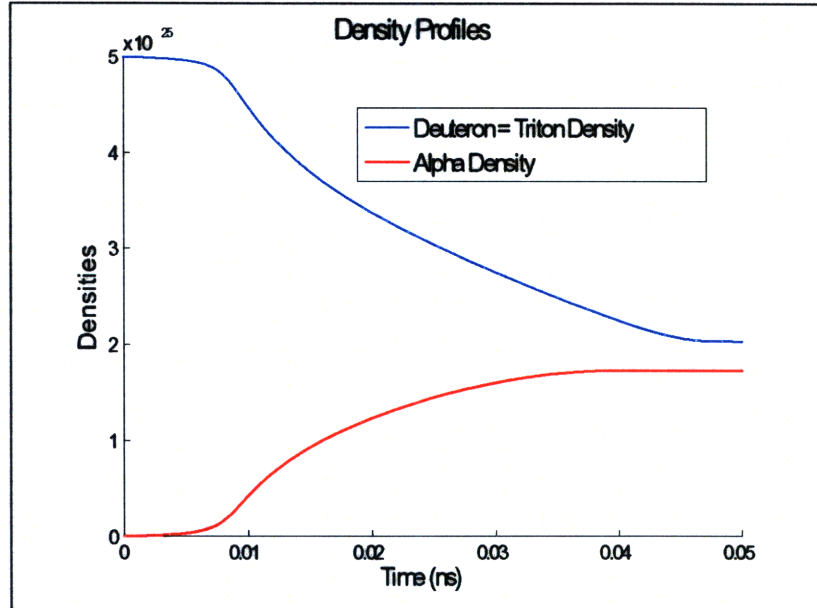


Figure 7: Densities (g/cm^3) of deuterium and tritium fuel ions and thermalized alpha particles

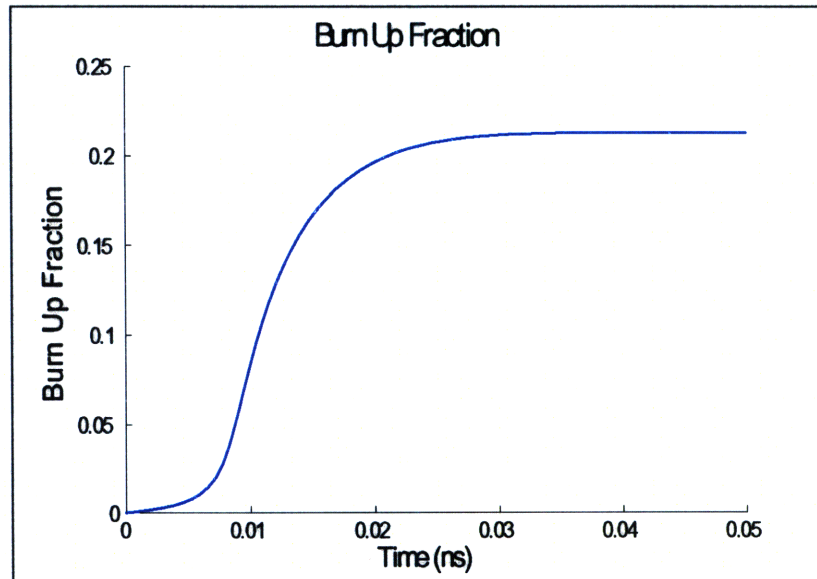


Figure 8: Burn Up Fraction

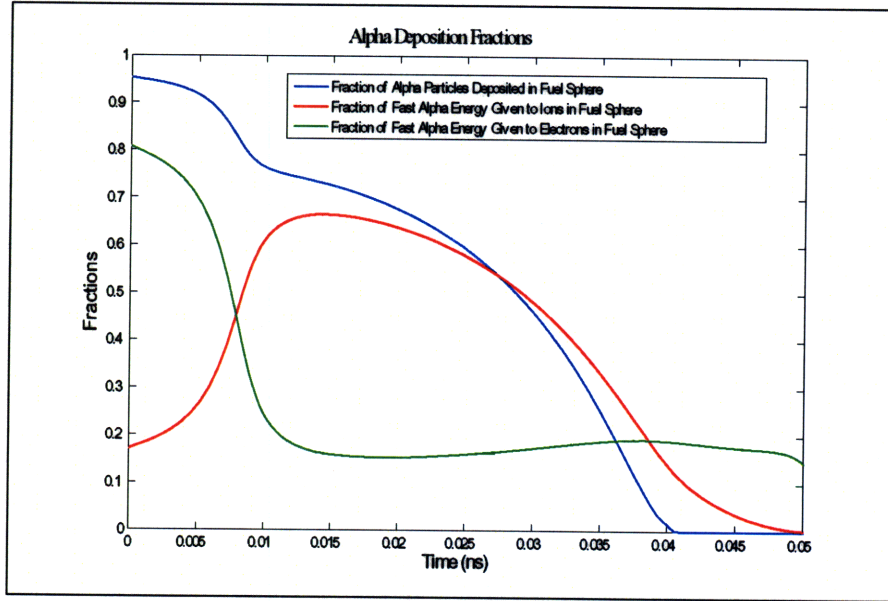


Figure 9: Fraction of fast alpha particles that are deposited in the fuel sphere (blue). Fraction of total instantaneous fusion power delivered to electrons (green). Fraction of total instantaneous fusion power delivered to ions (red).

fraction by the time runaway burn begins. Correspondingly, the fraction of alphas that stay in the fuel sphere $f_{n\alpha}$ decreases slowly until $t \approx 0.006$ ns. At this point, the rapidly increasing electron temperature (due to the high f_{ae}) increases the range of alpha particles ($R_\alpha \propto T_e^{3/2}$ for small T_e) resulting in a larger fraction of alphas that leave the fuel sphere. This can be seen by the fast decrease in $f_{n\alpha}$ at $t \approx 0.008$ ns. However, as the electron temperature continues to rise, the range of alpha particles 'saturates' due to ion collisions, and no longer goes like $T_e^{3/2}$. A brief plateau is seen in $f_{n\alpha}$ at $t \approx 0.01$ ns. At this point, the alpha particles predominantly heat the ions and the system enters the runaway burn regime. The rarefaction wave proceeds inwards quickly and the fraction of alpha particles deposited in the sphere continues to decline to zero at $t \approx 0.04$ ns. At this time the range of an alpha particle is greater than twice the fuel radius. The dropping electron temperature causes the electrons to be predominately heated by the alpha particles until the rarefaction wave reaches the origin at $t \approx 0.05$ ns. One can see from figure (8) that most of the

fuel is burned up between $t \approx 0.01$ and $t \approx 0.02$ seconds during the initial runaway. In the later stages of the burn, the volume of the fuel has been decreased considerably, and significant burnup does not occur. Time histories of the density within the fuel sphere are shown in figure (7). The final burnup fraction is 0.21.

Shown below are the same profiles but for the more marginal case with smaller burnup fraction. The initial conditions are $T_i = T_e = 5$ KeV, $R = 0.0126$ cm, $n_D = n_T = 1.42 \times 10^{25}$ #/cc, $\rho = 119$ g/cc, total mass $m = 1$ mg, and $\rho R = 1.5$ g/cm².

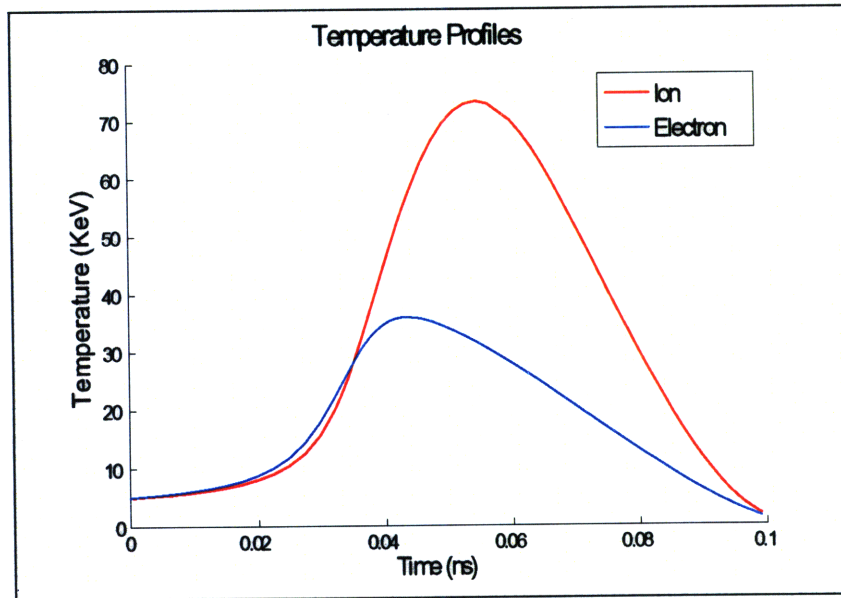


Figure 10: Ion and Electron Temperature Profiles

In this case, more of the alpha particles leave the system and the runaway burn is less pronounced. In the previous case the fraction of alpha particles deposited within the fuel sphere, $f_{n\alpha}$, briefly plateaued around $t \approx 0.01$ ns, whereas here there is no such effect. The fraction steadily declines to zero. Most of the energy that the ions receive is transferred at the end of the range of alpha particles (Bragg peak). When runaway burn begins to develop, too many alpha particles are leaving the system and the increase in ion energy fraction $f_{\alpha i}$ is marginal. The final burnup fraction in this case is 0.085.

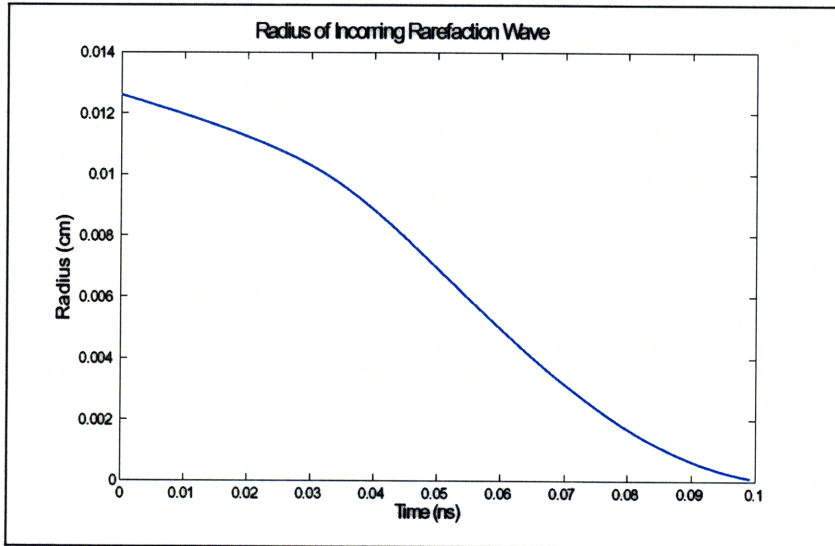


Figure 11: Radius of Incoming Rarefaction Wave

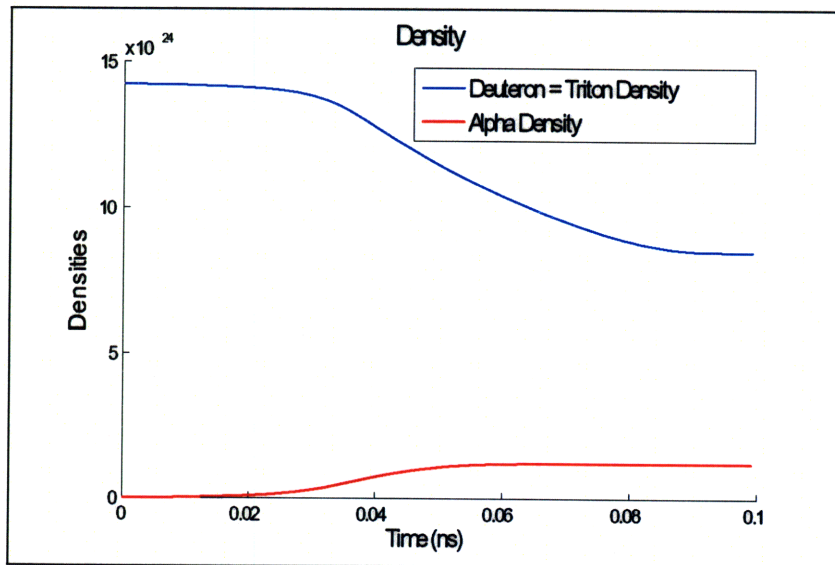


Figure 12: Densities (g/cm^3) of deuterium and tritium fuel ions and thermalized alpha particles

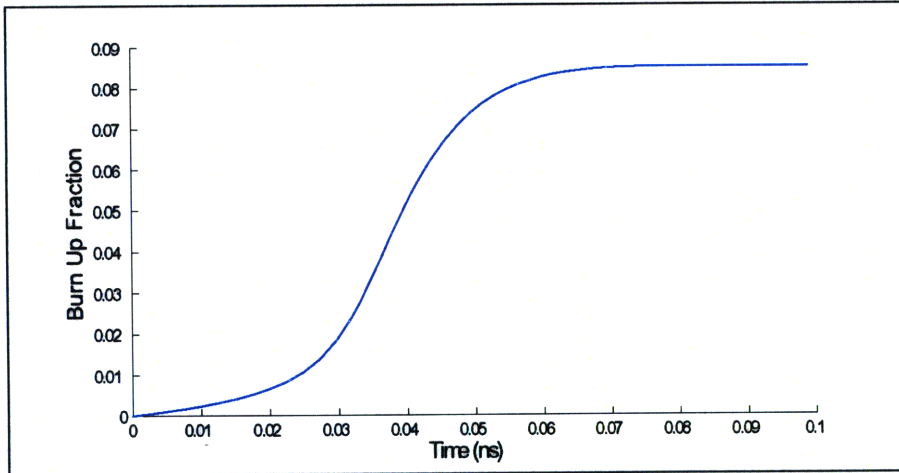


Figure 13: Burn Up Fraction

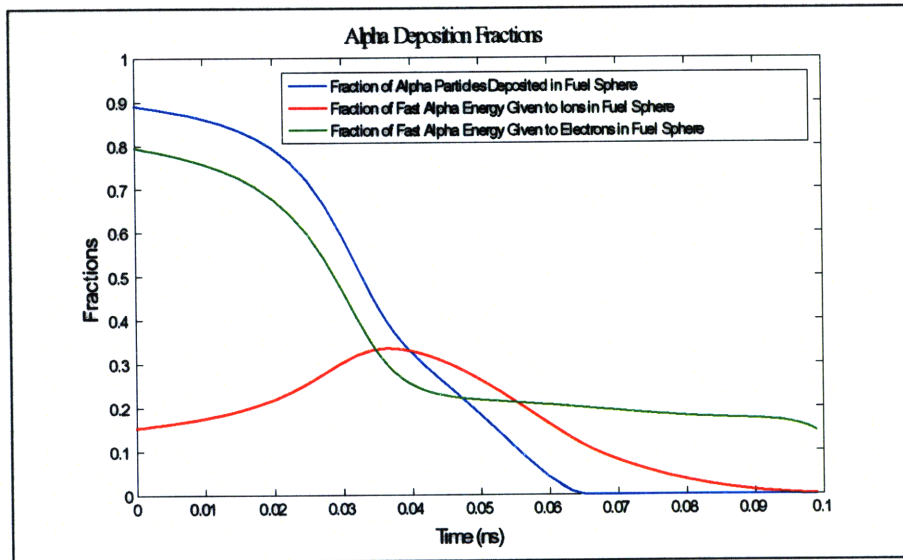


Figure 14: Fraction of fast alpha particles that are deposited in the fuel sphere (blue). Fraction of total instantaneous fusion power delivered to electrons (green). Fraction of total instantaneous fusion power delivered to ions (red).

The dependence of the fractional burnup on the initial fuel ρR will now be discussed. A common approximate formula for the burn up fraction was given by Fraley (Fraley *et al.* 1974)

$$Y = \frac{\rho R}{H_b + \rho R} \quad (226)$$

where ρR corresponds to the initial configuration. The burn parameter H_b is typically of the order 10. An expression for the burn parameter derived from simple considerations is given in Atzeni eq.(2.28), (Atzeni & Meyer-Ter-Vehn 2007)

$$H_b(T) = \sqrt{2T_i m_{eff}} \frac{8}{\langle \sigma v \rangle} \text{g/cm}^2 \quad (227)$$

Clearly, the larger the initial fuel ρR , the larger the burn fraction Y .

Another way to see the significance of ρR is to look at the alpha particle range. As seen in eq.(141), the range of an alpha particle scales inversely with the mass density of the fuel, $R_\alpha \propto 1/\rho$. If the range of alpha particles is small enough compared to the radius of the fuel sphere, the strong runaway burn regime can be reached. This can be seen in the two simulations above. In the marginal run, the fraction of alphas that stay in the sphere, $f_{n\alpha}$, was about 0.4 and was falling rapidly as the system was trying to undergo runaway burn. In the first run with larger ρR , not only was $f_{n\alpha} \approx 0.7$ as the ions began to run away, but $f_{n\alpha}$ had plateaued. The larger fraction of alpha particles remaining in the fuel $f_{n\alpha}$, and the plateauing effect of this fraction, play a key role in achieving higher burnup fractions. Therefore it is required that the following scaling hold

$$\rho R \propto \frac{R}{R_\alpha} > 1 \quad (228)$$

Using eq.(141) this can be made more explicit

$$\frac{R}{R_\alpha} = \frac{\ln(\Lambda)}{0.107 T_e^{3/2}} \rho R \approx 0.7 \rho R > 1. \quad (229)$$

where a value of $T_e \approx 15$, typical of electron temperatures right before runaway, was used. It is

then expected that for ρR 's greater than about 1.5, good burnup will occur, while for fuel spheres with $\rho R < 1.5$, burnup will be marginal. Note that for a real hot spot surrounded by cold dense fuel, ignition can occur for ρR 's smaller than 1. This is because the alpha particles that 'leave the sphere', or hot spot, get stopped a very short distance into the denser surrounding fuel. Their energy is not completely lost and can still effect the hot spot dynamics. Furthermore, the cold fuel acts as a tamper, and there is no rarefaction that occurs into the hot spot from the dense fuel at ignition.

Shown below in figure (15) is a plot of a series of burn fractions as a function of ρR for different initial temperatures and total fuel masses. The electron and ion initial temperatures were the same, and the mixtures were equimolar.

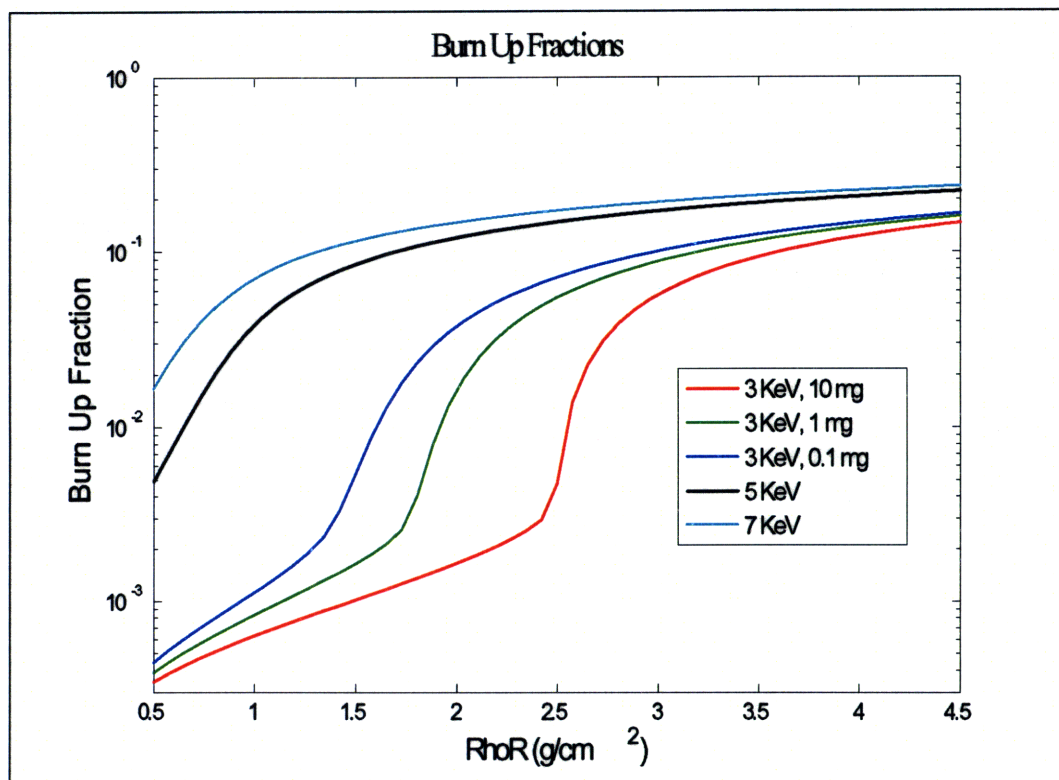


Figure 15: Burn up fractions as a function of ρR . The 5 KeV and 7 KeV initial temperature simulations were independent of initial fuel mass.

The two runs with initial temperatures of 5 and 7 KeV (turquoise and black curves) were the same for $m = 0.1, 1, \text{ and } 10 \text{ mg}$. For an initial temperature equal to 5 KeV or greater, the burn fraction does not depend on the initial fuel mass, only the initial ρR . Furthermore, as ρR increases, the burn fractions for the 5 and 7 KeV case approach each other. This behavior is expected from eq.(226) for $\rho R > H_b$. It is also seen that for $\rho R < 1.5$, the burn fractions begin to drop quickly.

However, there is clear mass dependence for the runs beginning at 3 KeV. This is due to the reabsorption of photons. The ideal ignition temperature for a pure homogenous DT fuel with only Bremsstrahlung emission is 4.7 KeV. This is well known in magnetic fusion, where reabsorption of photons is negligible. If photons are reabsorbed, less energy is lost from the fuel and the effective ignition temperature is lowered. In the limit where the fuel is very optically thick, then no photons will be lost from the system (aside from the boundaries). The radiation field will tend to build up toward a black body, or possibly diluted Planckian(Molvig *et al.* 2009). If there is enough total energy input from fusion (and/or other sources) to raise the matter and black body radiation to over 5 KeV, the system can run away. The average reabsorption mean free path is inversely proportional to the matter density, $l_p \propto 1/\rho$. However, $\rho \propto (\rho R)^{3/2} / \sqrt{m}$. Therefore, fuel spheres with a larger mass for a given ρR will have a larger re-absorption mean free path. More energy will leave the system and runaway burn may not be as pronounced. This behavior is seen in the figure (15) where there are clear 'yield cliffs' located at different ρR for the different masses. The burn fraction of the lower mass run increases sharply at $\rho R \approx 1.5$, while the burn fraction of the higher mass run increases sharply at $\rho R \approx 2.5$. For larger ρR the burn fractions approach the same value.

The curves shown in figure (15) do not exactly match the functional form of eq.(226). However, the large ρR limit of the 5 and 7 KeV runs are consistent with $H_b \approx 14$. Evaluation of the burn parameter in equation (227) gives $H_b = 19$ for $T = 5 \text{ KeV}$ and $H_b = 7.3$ for $T = 7 \text{ KeV}$.

7 Conclusion

The goal of this thesis was to develop a system of ODE equations that model essential features of the burn of compressed ICF fuel capsules, and that can be integrated faster than most one or two

dimensional radiation hydrocodes. Particular attention was given to burn physics, the treatment of the slowing down of fast alpha particles, and the theory developed was then applied to the isothermal rarefaction model. Many effects were seen in the simulations using this model such as runaway burn, strong preferential heating of ions or electrons, effects of photon reabsorption, yield cliffs, and dependence of burn up on ρR . This model can be used as an effective quick estimate of the performance of a compressed ICF capsule.

The most significant drawback of this model is that it is zero-D and assumes a homogenous state. The code does not model hot spot ignition, which is seen as a necessity by most. In real capsules, significant burn may occur while the whole fuel is very non-isothermal. An understanding and ability to simulate hot spot ignition and burn propagation are essential for a detailed ICF design. Furthermore, the radiation transport is simplified in that scattering and explicit time dependence is ignored. Scattering can be important even in the near-thin limit, and in cases where the diffusion approximation is valid, explicit time dependence definitely cannot be ignored.

However, the theory developed here can readily be applied to more sophisticated codes which have explicit spatial dependence. For instance, an explicit 1-D code can integrate alpha particles along a certain number of rays from every cell in the geometry using equation (124) to find the fusion source and sink terms for each cell for each time step. Each cell can be considered homogenous. Advection, diffusion, and viscous terms in the momentum and energy equations would have to be added. A more sophisticated radiation treatment could be added as well, although in many cases assuming pure Bremsstrahlung emission is not that bad of an approximation.

Bibliography

- Atzeni, Stefano & Meyer-Ter-Vehn, Jurgen, *The Physics of Inertial Fusion* (Oxford: Oxford University Press, 2007).
- Bosch, H.S. & Hale, G.M., *Nucl. Fusion*, vol. 32, 611 (1992).
- Chen, Francis F., *Introduction to Plasma Physics and Controlled Fusion* (New York, NY: Springer, 2006).
- Fraley, G. S., Linnebur, E. J., Mason, R. J. & Morse, R. L., *Phys. Fluids*, vol. 17, 474 (1974).
- Helander, Per & Sigmar, Dieter J., *Collisional Transport in Magnetized Plasmas* (Cambridge, UK: Cambridge University Press, 2002).
- Jose M. Martinez-Val, Guillermo Velarde, Yigal Ronen, *An Introduction to Nuclear Fusion by Inertial Confinement* (Boca Raton, Florida: CRC Press, Inc., 1993).
- Kompaneets, A.S., *Soviet Phys. JETP*, vol. 4, 730 (1957).
- Krokhin, O. N. & Rozanov, V. B., *Soviet Journal of Quantum Electronics*, vol. 2, 393–394 (1973).
- Molvig, Kim, Alme, Marv, Webster, Robert & Galloway, Conner, *Physics of Plasmas*, vol. 16, 023301 (2009).
- Zel'dovich, Ya. B. & Raizer, Yu. P., *Physics of Shock Waves and High-Temperature Hydrodynamic Phenomena* (Mineola, New York: Dover Publications, Inc., 2002).